Supporting Information

(Thio)Ureido Anion Receptors Based on a 1,3-Alternate Oxacalix[2]arene[2]pyrimidine Scaffold

Wim Van Rossom,[†] Jef Caers,[†] Koen Robeyns,[‡,§] Luc Van Meervelt,[‡] Wouter Maes,*[,†,⊥] and Wim Dehaen*[,†]

[†] Molecular Design and Synthesis, Department of Chemistry, Katholieke Universiteit Leuven (KU Leuven), Celestijnenlaan 200F, 3001 Leuven, Belgium
[‡] Biomolecular Architecture, Department of Chemistry, Katholieke Universiteit Leuven (KU Leuven), Celestijnenlaan 200F, 3001 Leuven, Belgium
[§] Institute of Condensed Matter and Nanosciences (IMCN), Université Catholique de Louvain (UCL), Bâtiment Lavoisier, place Louis Pasteur 1, bte 3, 1348 Louvain-la-Neuve, Belgium
[⊥] Design & Synthesis of Organic Semiconductors (DSOS), Institute for Materials Research (IMO-IMOMEC), Hasselt University, Agoralaan 1 – Building D, 3590 Diepenbeek, Belgium

wim.dehaen@chem.kuleuven.be; wouter.maes@uhasselt.be

Table of Contents

1. ^{1}H and ^{13}C NMR spectra

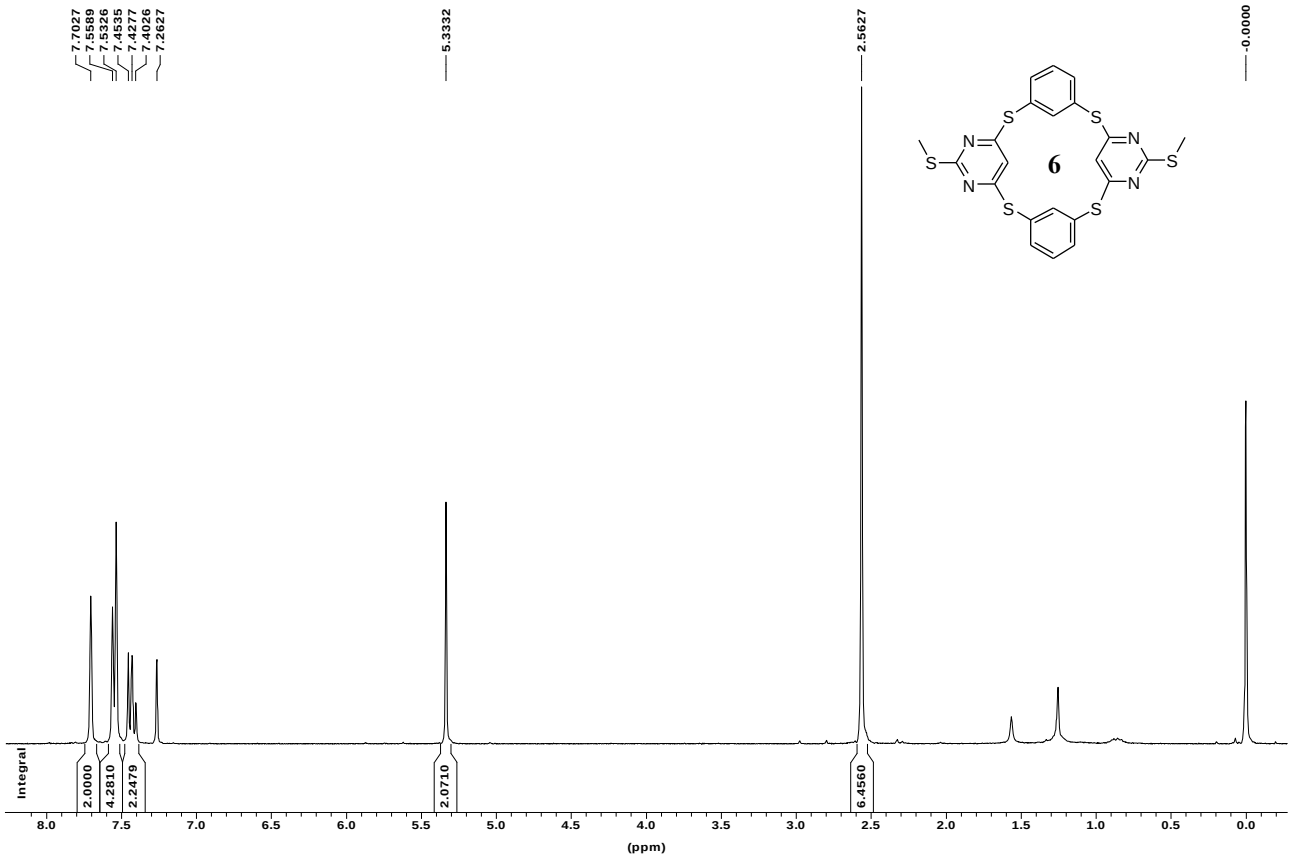

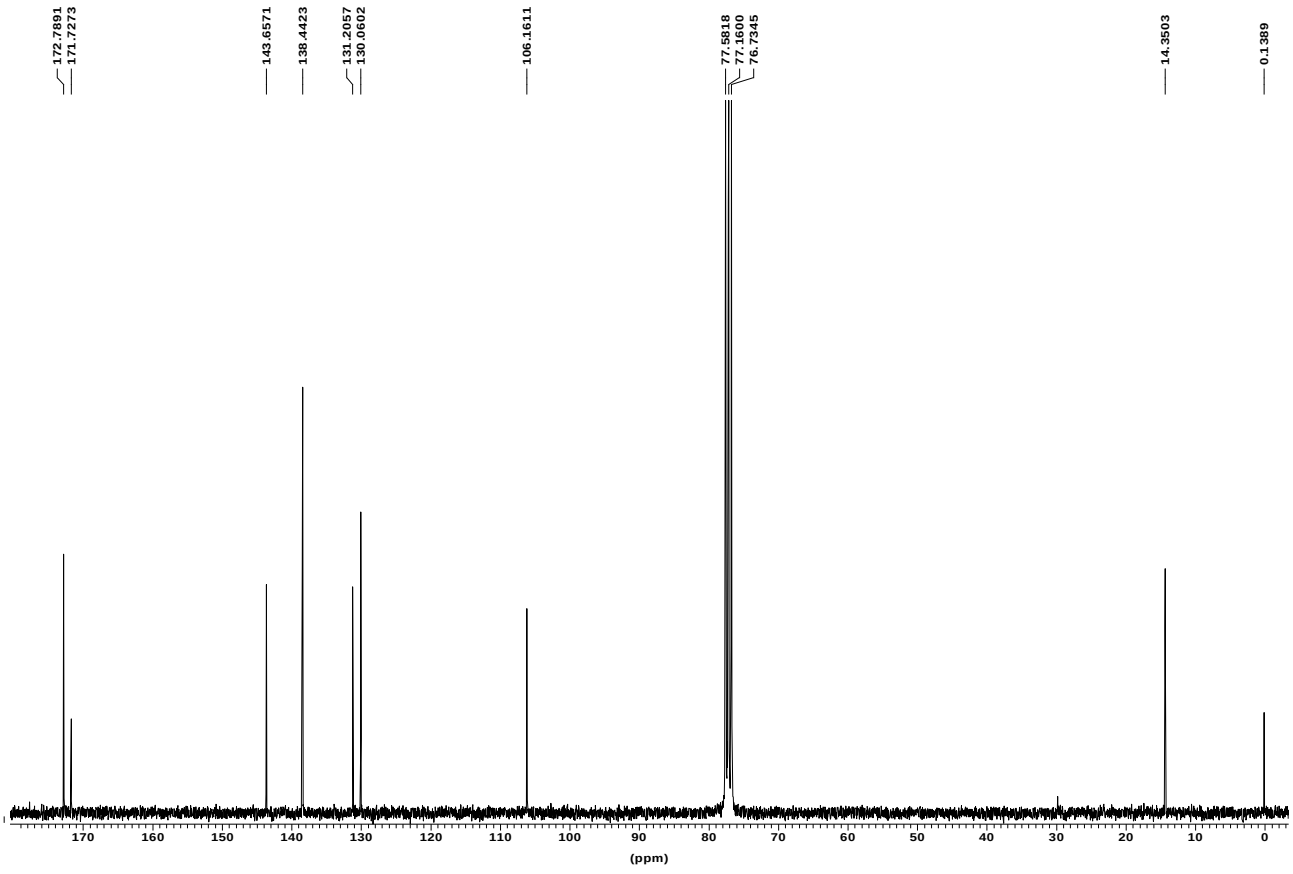

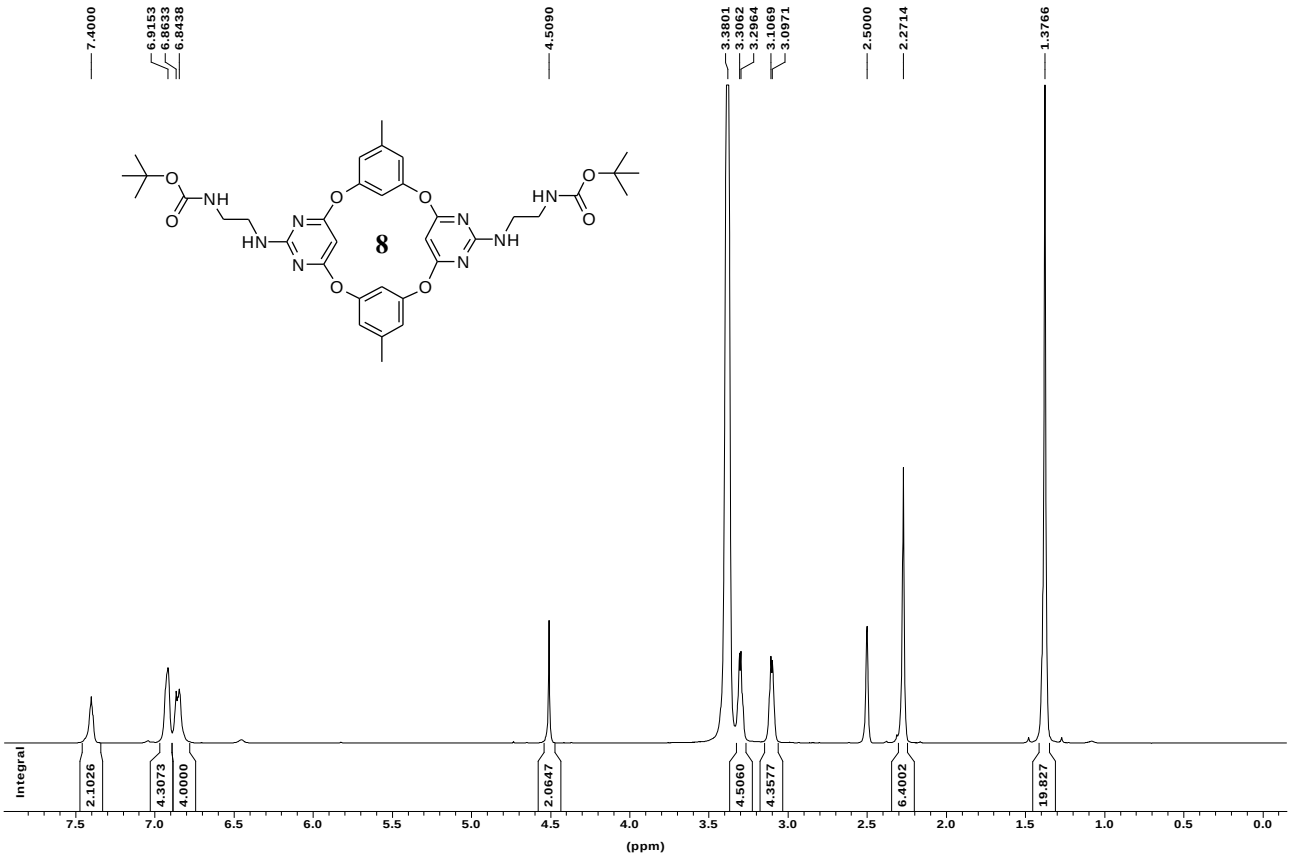
7.4000
6.9153
6.8633
6.8438
4.5090
3.3801
3.3062
3.2964
3.1069
3.0971
2.5000
2.2714
1.3766
8
Integral
2.1026
4.3073
4.0000
2.0647
4.5060
4.3577
6.4002
19.827
(ppm)

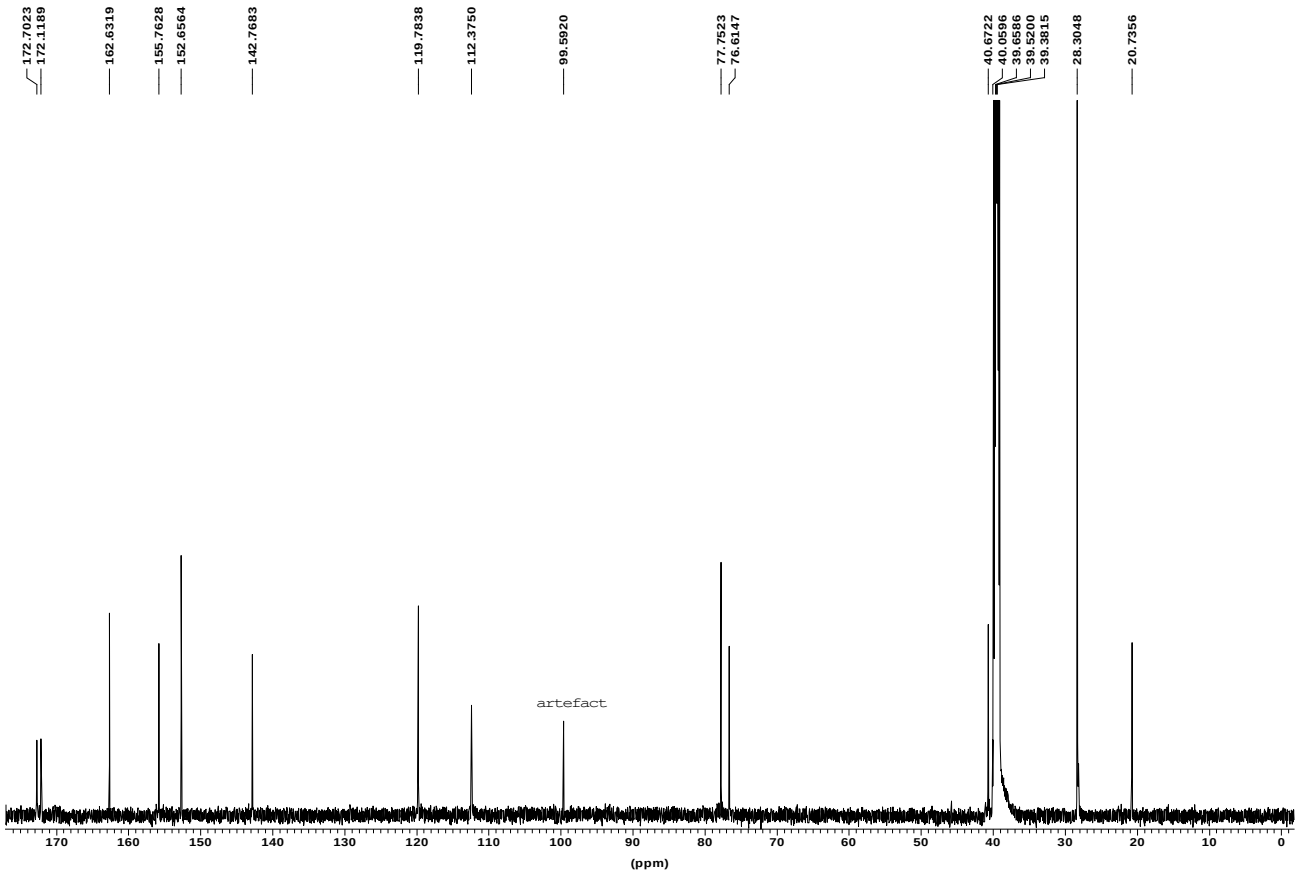
172.7023
172.1189
162.6319
155.7628
152.6564
142.7683
119.7838
112.3750
99.5920
77.7523
76.6147
40.6722
40.0596
39.6586
39.5200
39.3815
28.3048
20.7356
artefact
(ppm)

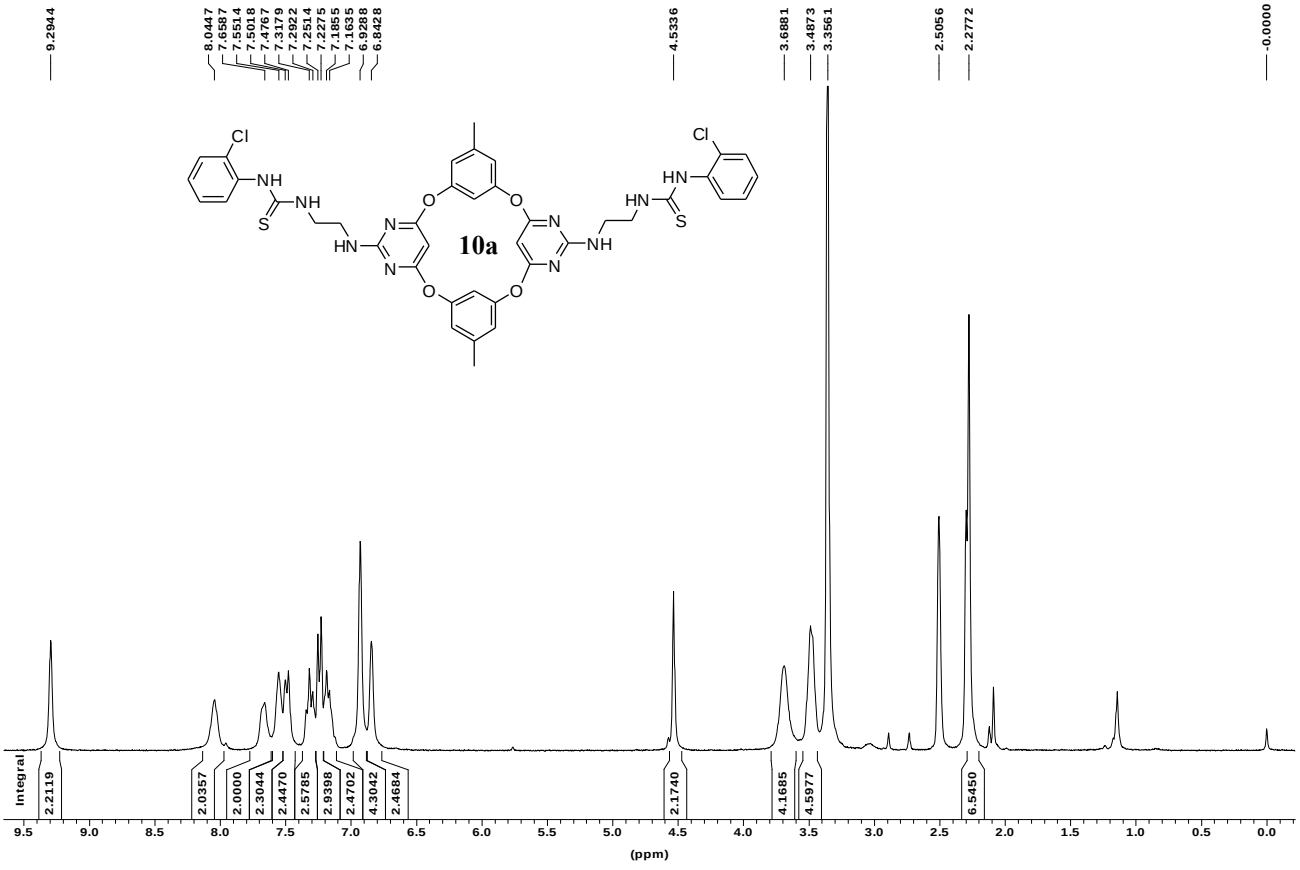
9.2944
8.0447
7.6587
7.5514
7.5018
7.4767
7.3179
7.2922
7.2514
7.2275
7.1885
7.1635
6.9288
6.8428
4.5336
3.6881
3.4873
3.3561
2.5056
2.2772
-0.0000
Cl
NH
S
NH
HN
N
N
O
O
O
O
N
N
HN
NH
S
HN
Cl
10a
Integral
2.2119
2.0357
2.0000
2.3044
2.4470
2.5785
2.9398
2.4702
4.3042
2.4684
2.1740
4.1685
4.5977
6.5450
(ppm)

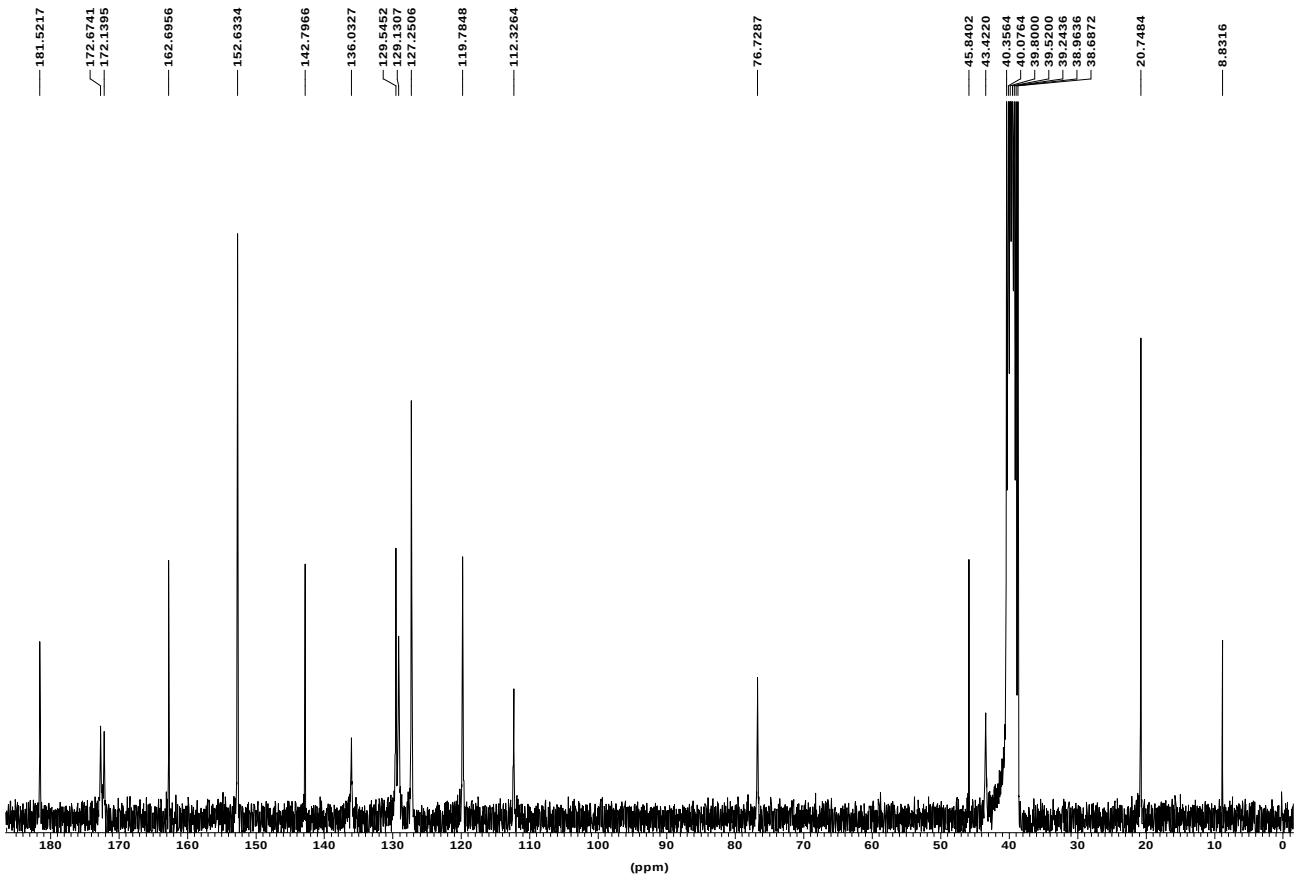
181.5217
172.6741
172.1395
162.6956
152.6334
142.7966
136.0327
129.5452
129.1307
127.2506
119.7848
112.3264
76.7287
45.8402
43.4220
40.3564
40.0764
39.8000
39.5200
39.2436
38.9636
38.6872
20.7484
8.8316
(ppm)

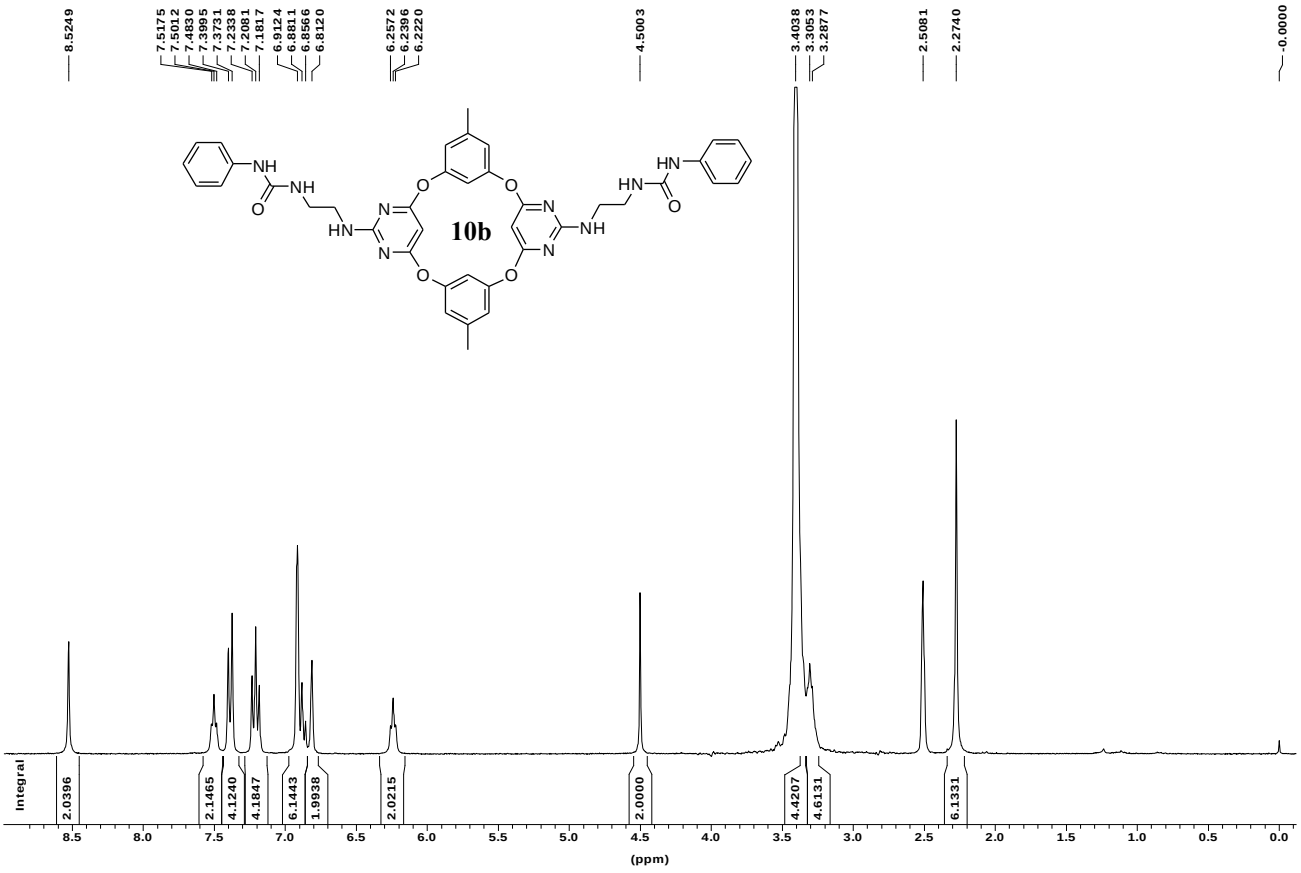
8.5249
7.5175
7.5012
7.4830
7.3995
7.3731
7.2338
7.2081
7.1817
6.9124
6.8811
6.8566
6.8120
6.2572
6.2396
6.2220
4.5003
3.4038
3.3053
3.2877
2.5081
2.2740
-0.0000
10b
Integral
2.0396
2.1465
4.1240
4.1847
6.1443
1.9938
2.0215
2.0000
4.4207
4.6131
6.1331
(ppm)

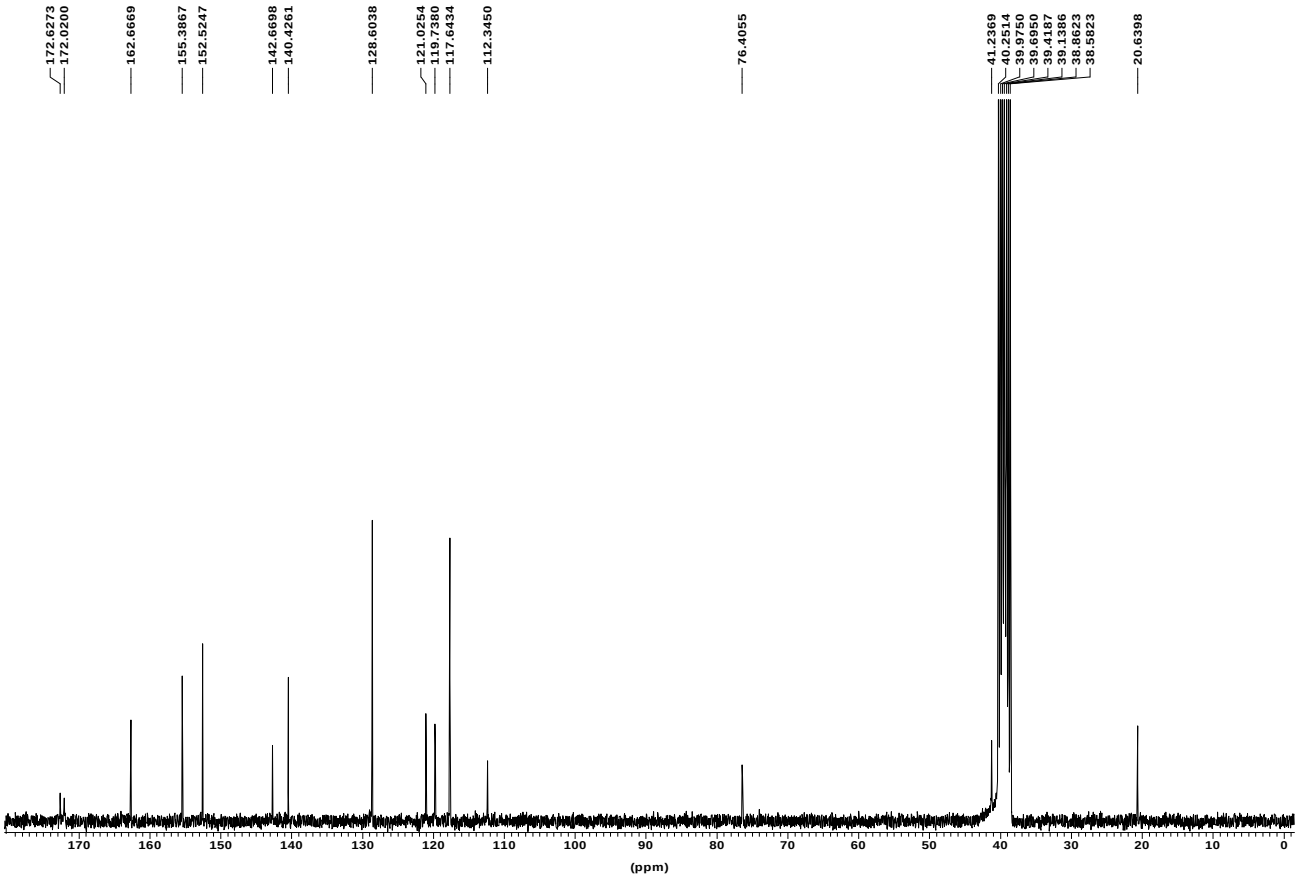
172.6273
172.0200
162.6669
155.3867
152.5247
142.6698
140.4261
128.6038
121.0254
119.7380
117.6434
112.3450
76.4055
41.2369
40.2514
39.9750
39.6950
39.4187
39.1386
38.8623
38.5823
20.6398
(ppm)

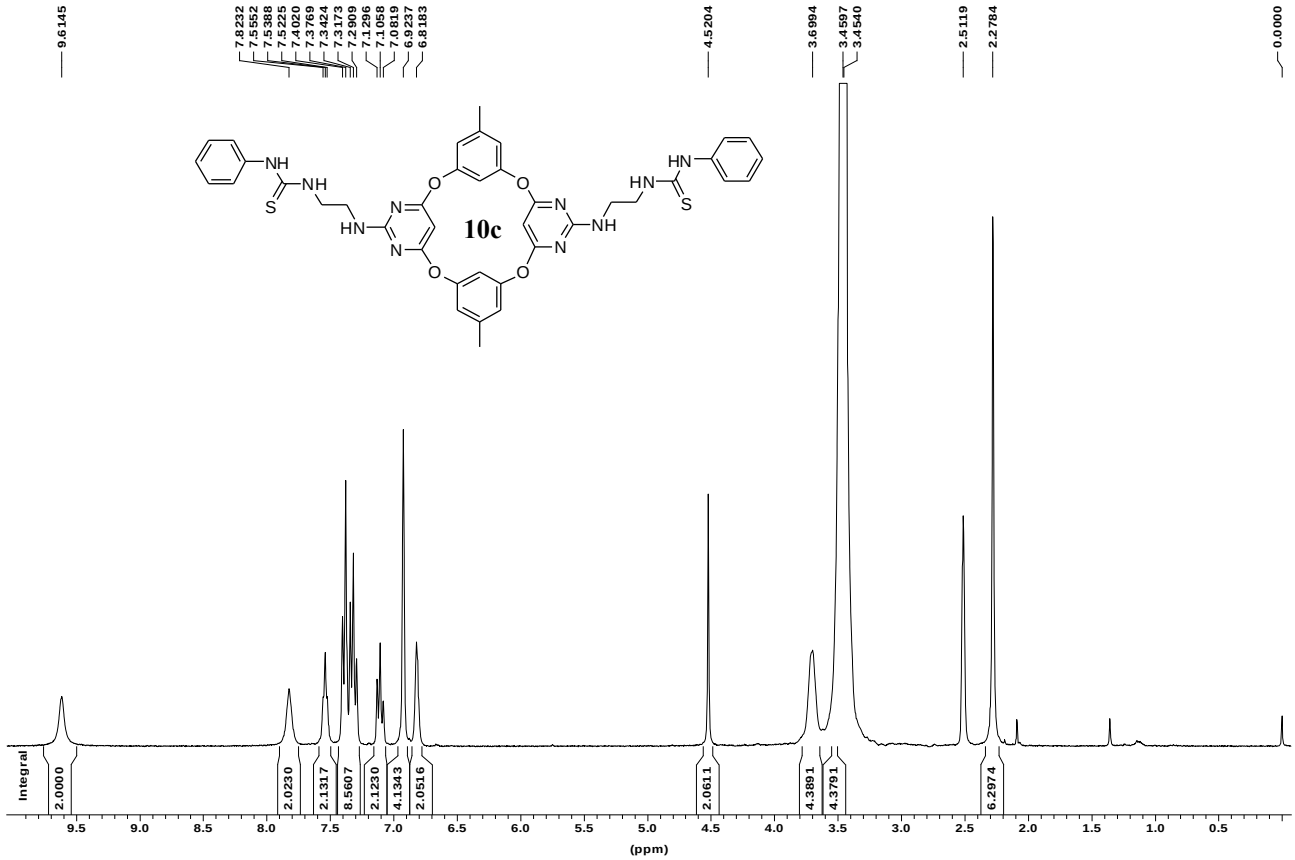
9.6145
7.8232
7.5552
7.5388
7.5225
7.4020
7.3769
7.3424
7.3173
7.2909
7.1296
7.1058
7.0819
6.9237
6.8183
4.5204
3.6994
3.4597
3.4540
2.5119
2.2784
0.0000
10c
Integral
2.0000
2.0230
2.1317
8.5607
2.1230
4.1343
2.0516
2.0611
4.3891
4.3791
6.2974
(ppm)

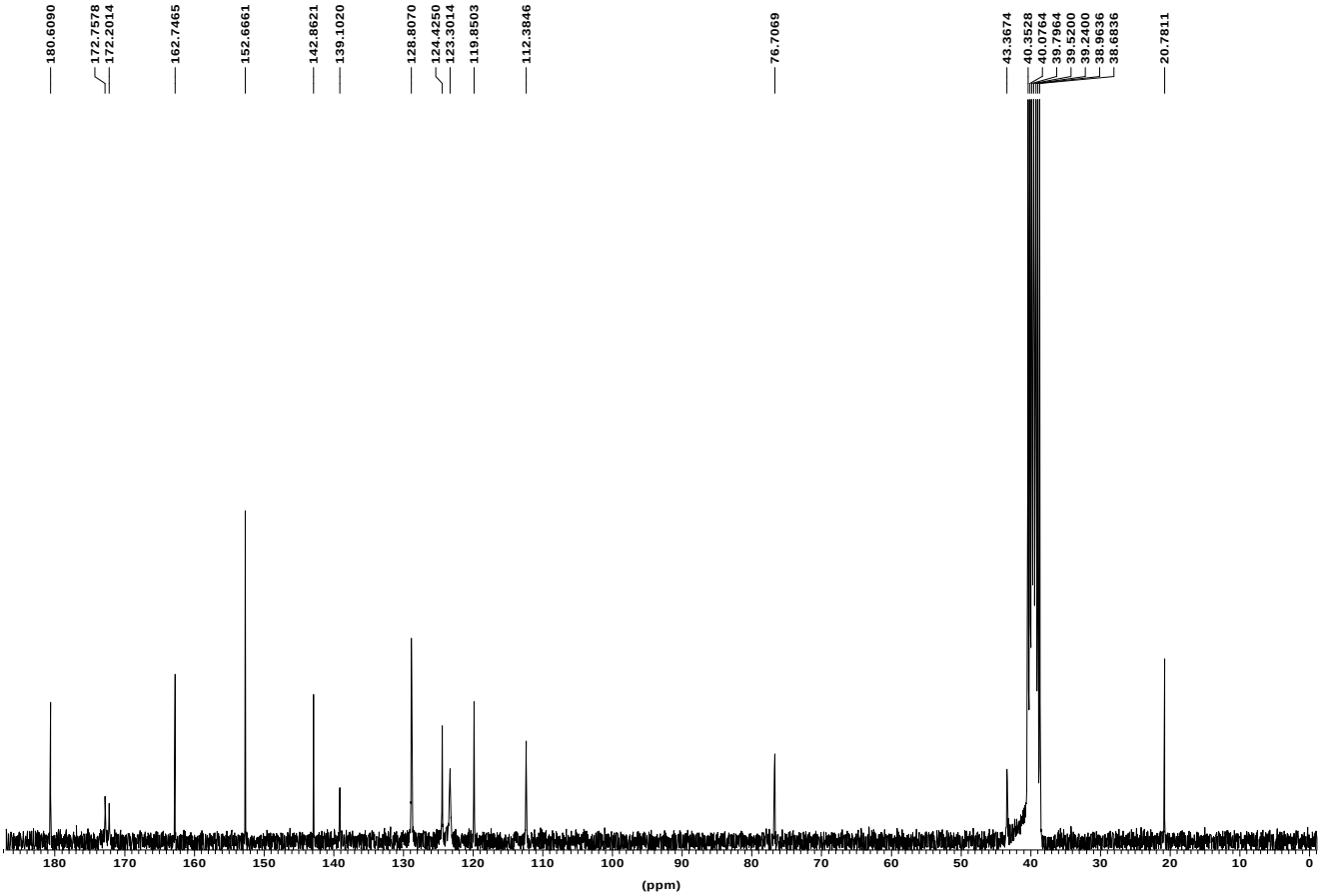
180.6090
172.7578
172.2014
162.7465
152.6661
142.8621
139.1020
128.8070
124.4250
123.3014
119.8503
112.3846
76.7069
43.3674
40.3528
40.0764
39.7964
39.5200
39.2400
38.9636
38.6836
20.7811
(ppm)

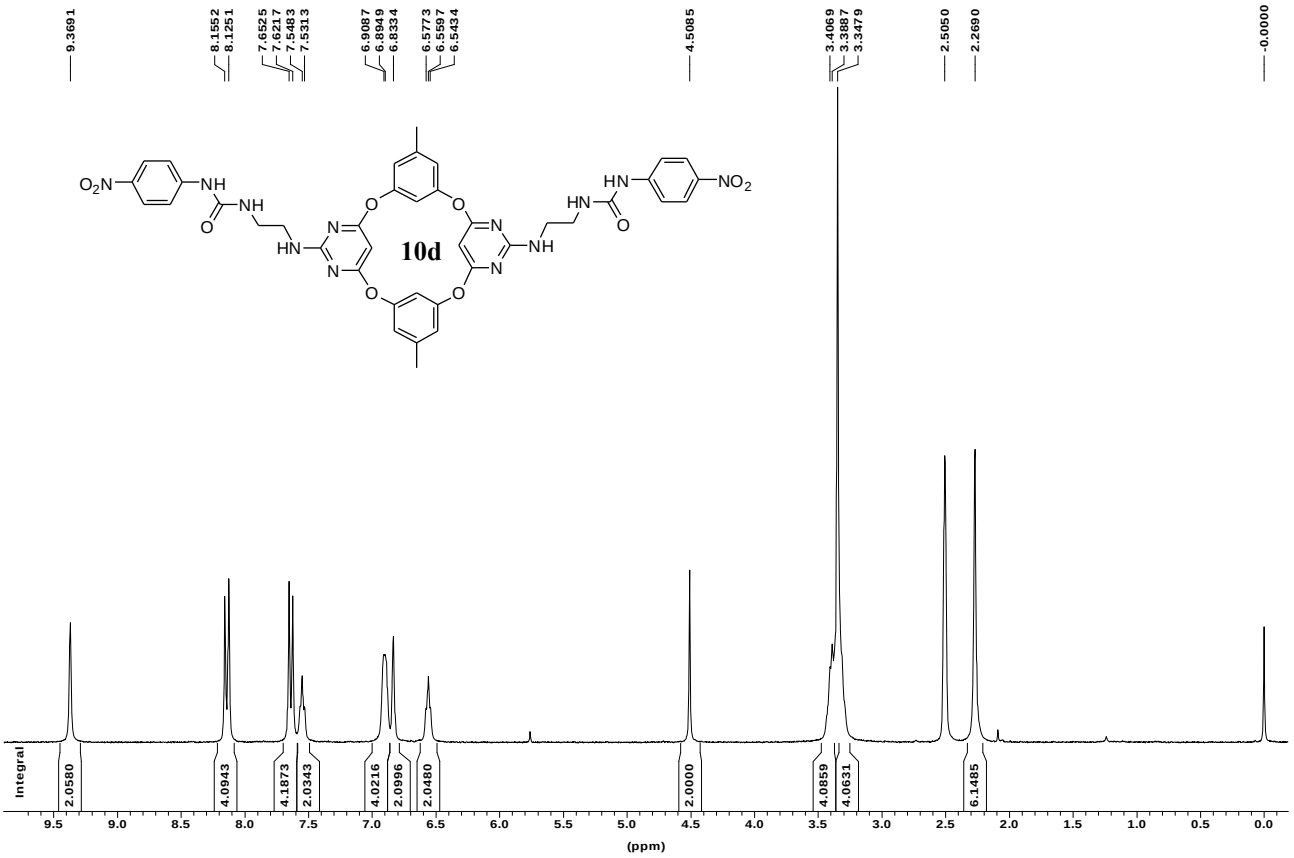
9.3691
8.1552
8.1251
7.6525
7.6217
7.5483
7.5313
6.9087
6.8949
6.8334
6.5773
6.5597
6.5434
4.5085
3.4069
3.3887
3.3479
2.5050
2.2690
-0.0000
10d
Integral
2.0580
4.0943
4.1873
2.0343
4.0216
2.0996
2.0480
2.0000
4.0859
4.0631
6.1485
(ppm)

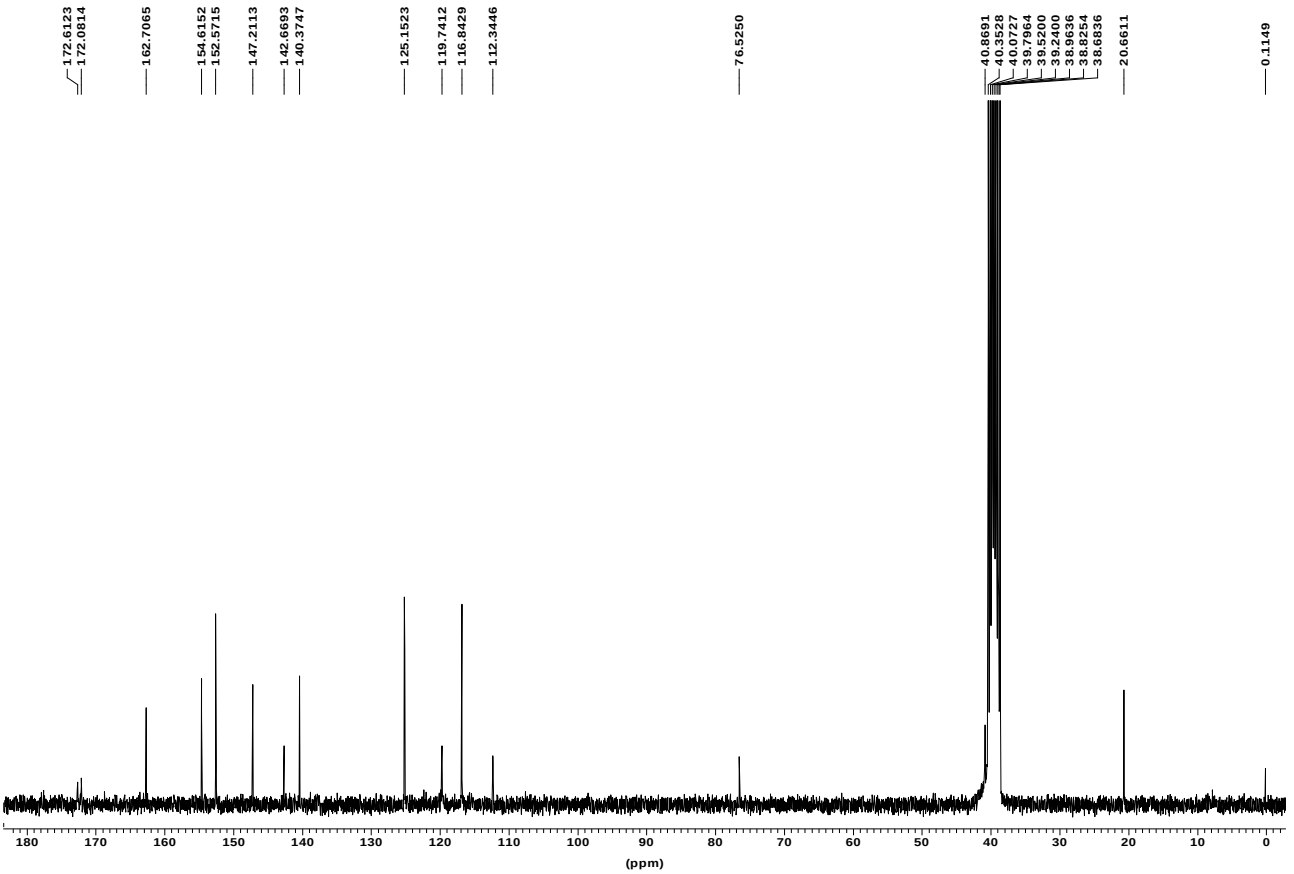
172.6123
172.0814
162.7065
154.6152
152.5715
147.2113
142.6693
140.3747
125.1523
119.7412
116.8429
112.3446
76.5250
40.8691
40.3528
40.0727
39.7964
39.5200
39.2400
38.9636
38.8254
38.6836
20.6611
0.1149
(ppm)

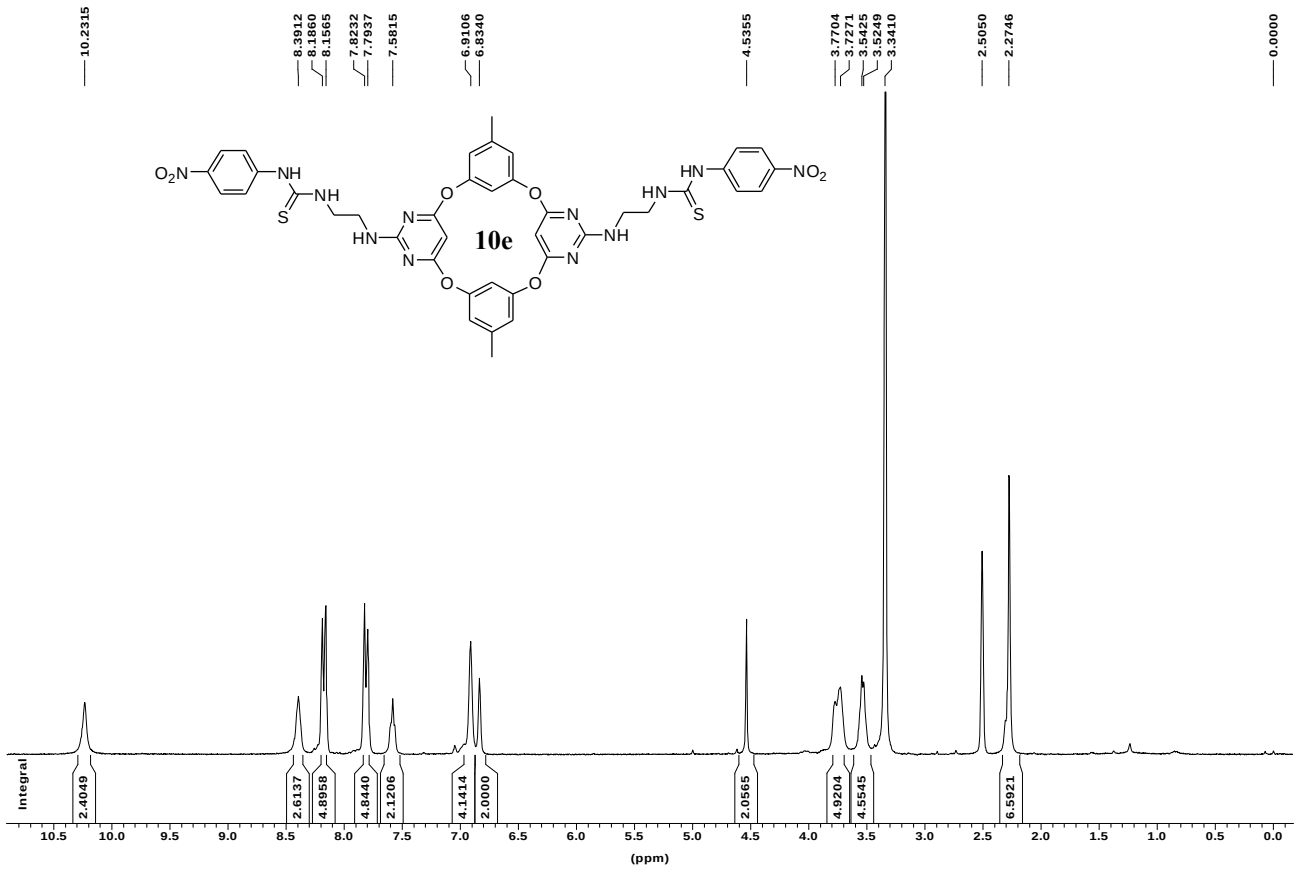
10.2315
8.3912
8.1860
8.1565
7.8232
7.7937
7.5815
6.9106
6.8340
4.5355
3.7704
3.7271
3.5425
3.5249
3.3410
2.5050
2.2746
0.0000
10e
Integral
2.4049
2.6137
4.8958
4.8440
2.1206
4.1414
2.0000
2.0565
4.9204
4.5545
6.5921
(ppm)

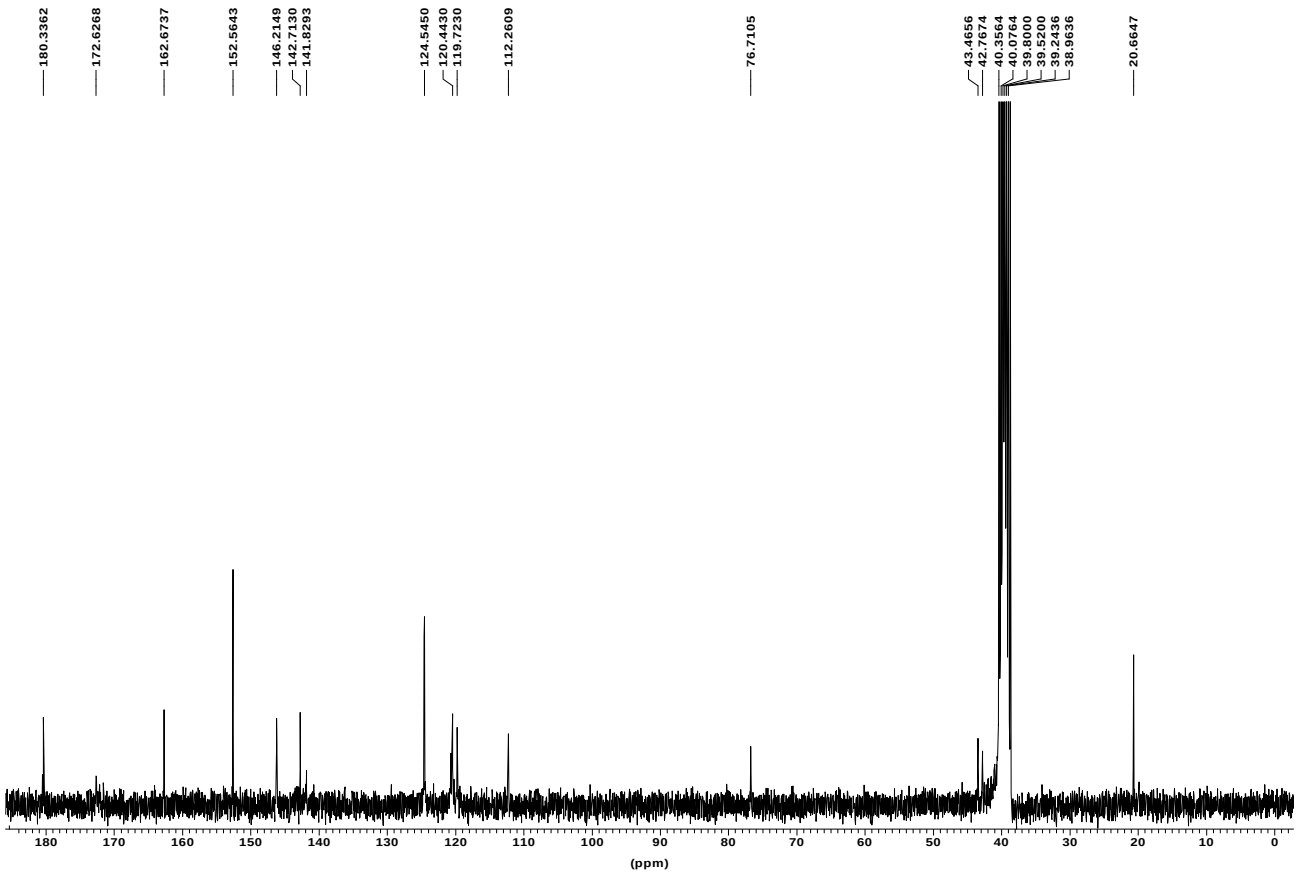
180.3362
172.6268
162.6737
152.5643
146.2149
142.7130
141.8293
124.5450
120.4430
119.7230
112.2609
76.7105
43.4656
42.7674
40.3564
40.0764
39.8000
39.5200
39.2436
38.9636
20.6647
(ppm)

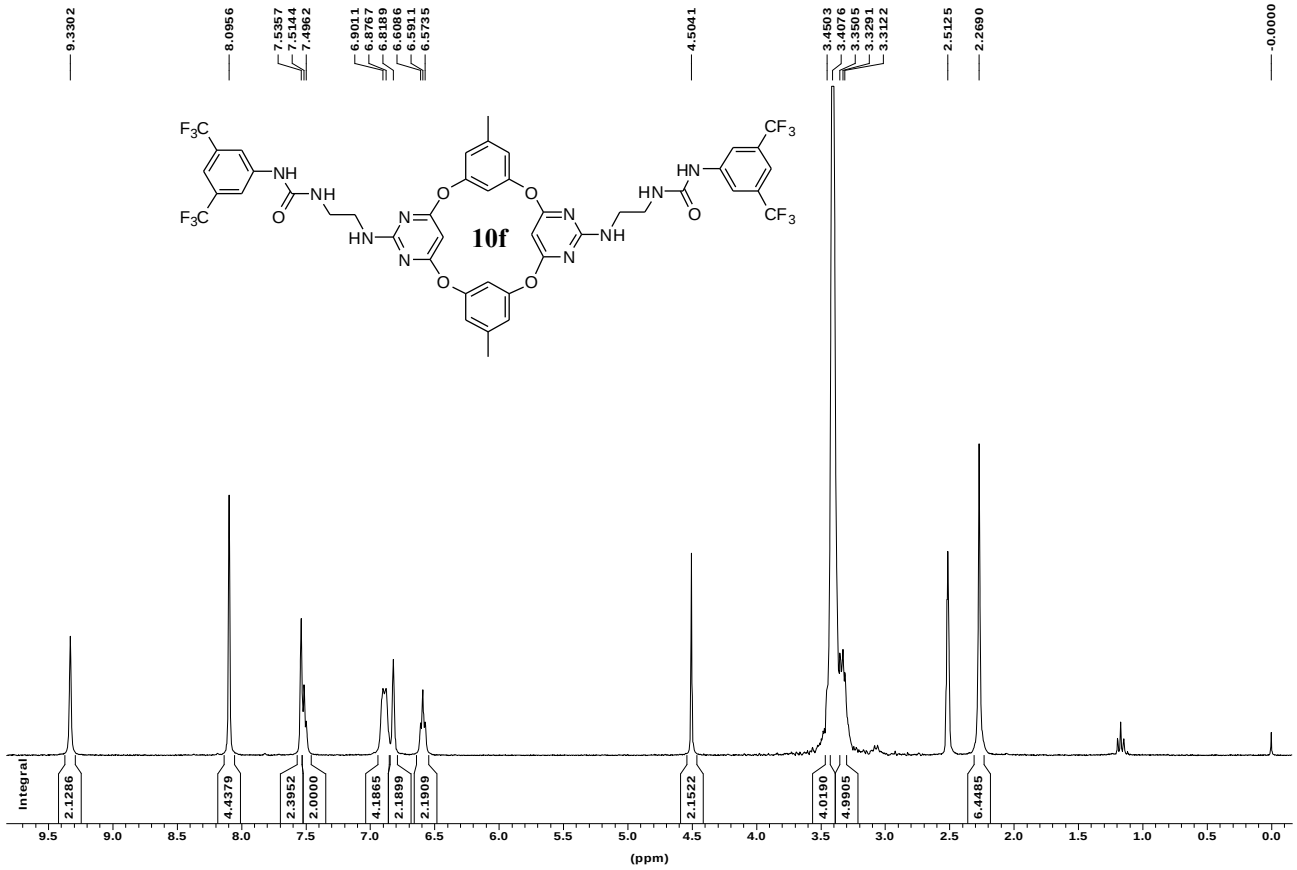
9.3302
8.0956
7.5357
7.5144
7.4962
6.9011
6.8787
6.8189
6.6086
6.5911
6.5735
4.5041
3.4503
3.4076
3.3505
3.3291
3.3122
2.5125
2.2690
-0.0000
10f
Integral
2.1286
4.4379
2.3952
2.0000
4.1865
2.1899
2.1909
2.1522
4.0190
4.9905
6.4485
(ppm)

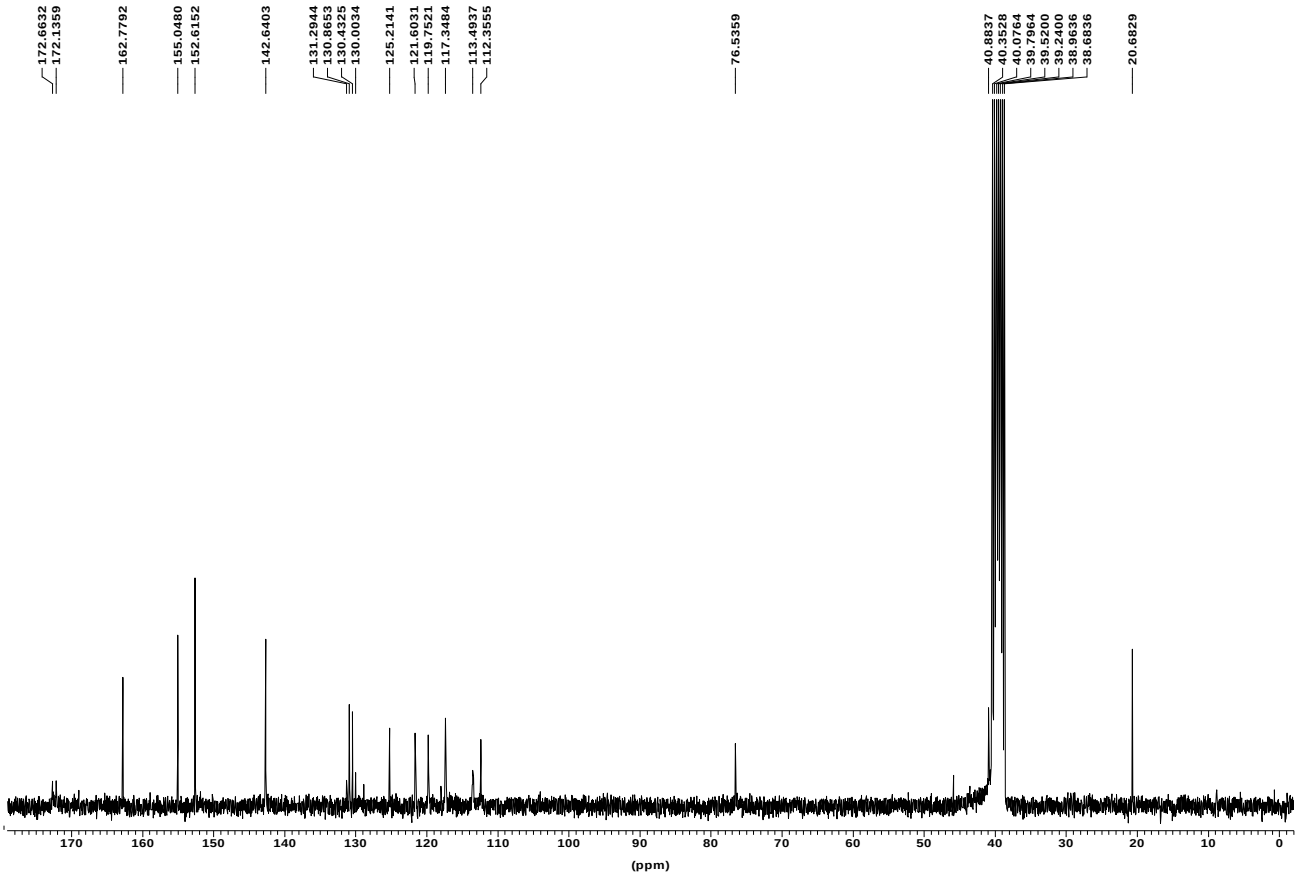
172.6632
172.1359
162.7792
155.0480
152.6152
142.6403
131.2944
130.8653
130.4325
130.0034
125.2141
121.6031
119.7521
117.3484
113.4937
112.3555
76.5359
40.8837
40.3528
40.0764
39.7964
39.5200
39.2400
38.9636
38.6836
20.6829
(ppm)

2. X-ray crystallographic data and additional figures for heteracalix[2]arene[2]pyrimidines 3 and 6

The crystals of **3**, grown by vapor diffusion of pentane into a $CHCl_3$ solution of the macrocycle (at rt), belong to the triclinic space group *P*-1. A colorless transparent crystal with approximate dimensions of 0.35x0.25x0.20 mm was selected for data collection using monochromated (Göbel mirrors) CuKα radiation (λ = 1.54178 Å) and phi and omega scans. Data were collected at a temperature of 100 K on a SMART 6000 diffractometer equipped with a CCD detector. Cell refinement and data reduction were carried out by the program SAINT[1] on a total of 12469 reflections (4861 independent reflections, R_{int} = 8.72%). The structure was solved by direct methods (SHELXS) and refined by full-matrix least squares on $|F^2|$ using the SHELXTL program package,[2] converging to a final $R_1 = 0.0663$, $\omega R_2 = 0.1585$ for 3285 reflections with $I_o > 2\sigma(I_o)$ and GOOF = 1.013. Non-hydrogen atoms were anisotropically refined and the hydrogen atoms were placed on calculated positions with temperature factors fixed at 1.2 times U_{eq} of the parent atoms and 1.5 times U_{eq} for methyl groups. The fundamental crystal data and experimental parameters for the structure determination are summarized below.

formula	$C_{24}H_{20}N_4O_4S_2$, $CHCl_3$
M (gmol^{-1})	611.93
crystal dimensions (mm^3)	0.35x0.25x0.20
crystal system	Triclinic
space group	*P*-1
a (Å)	10.7931(13)
b (Å)	11.7407(12)
c (Å)	12.4871(12)
α (deg)	116.859(5)
β (deg)	104.689(7)
γ (deg)	93.089(5)
V (Å^3)	1374.3(3)
Z	2
ρ_{calc} (gcm^{-3})	1.479
$2\theta_{max}$ (deg)	69.72
radiation	CuKα
λ (Å)	1.54178
F(000)	628
T (K)	100(2)
measured reflections	12469
unique reflections	4861
observed reflections ($I_o > 2\sigma(I_o)$)	3285
parameters refined	375
R_1	0.0663
ωR_2[a]	0.1585
R_1 (all data)	0.1067
ωR_2 (all data)	0.1810
GOOF	1.013
μ (mm^{-1})	4.778

[a] Weighting scheme as defined for this component: $\omega = 1 / [\sigma^2(F_o^2) + (0.0000\ P)^2 + 0.3014\ P]$, $P = (F_o^2 + 2F_c^2) / 3$

[1] SAINT, Manual Version 5/6.0, Bruker Analytical X-ray systems Inc.: Madison, 1997.
[2] Sheldrick G. M. *Acta Crystallogr. A* **2008**, *64*, 112.

The difference in C-O bond distances of the bridging oxygen atoms confirmed the electrophilic character of the pyrimidine rings (mainly conjugation to the neighboring pyrimidine components). On average, the C-O bond is 0.043 Å shorter toward the pyrimidine (<1.354 Å>; range 1.346(4)–1.359(5) Å) than toward the benzenoid (<1.397 Å>; range 1.387(4)–1.411(4) Å) ring (Figure S1). The short contacts (3.285 Å) in the packing between neighboring pyrimidine rings of different calixarene molecules can be considered as weak π-π interactions.

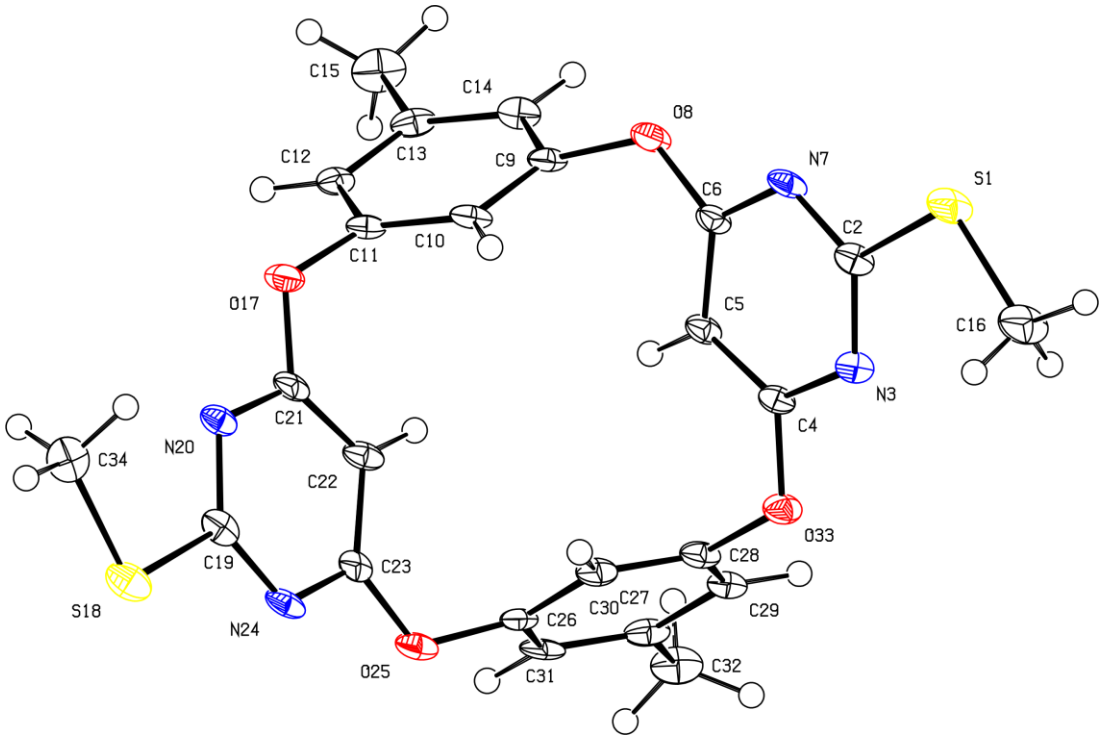

Figure S1. Single-crystal structure for oxacalix[4]arene **3**, showing displacement ellipsoids drawn at the 50% probability level ($CHCl_3$ not shown).

The crystals of thiacalix[4]arene **6**, also grown by vapor diffusion of pentane into a $CHCl_3$ solution of the macrocycle (at rt), belong to the monoclinic space group *C*2/c. A colorless transparent crystal with approximate dimensions of 0.5x0.3x0.15 mm was selected for data collection using monochromated (Göbel mirrors) CuKα radiation (λ = 1.54178 Å) and phi and omega scans. Data were collected at a temperature of 100 K on a SMART 6000 diffractometer equipped with a CCD detector. Cell refinement and data reduction were carried out by the program SAINT[1] on a total of 13282 reflections (2692 independent reflections, R_{int} = 8.72%). The structure was solved by direct methods (SHELXS) and refined by full-matrix least squares on $|F^2|$ using the SHELXTL program package,[2] converging to a final R_1 = 0.0480, ωR_2 = 0.0999 for 2692 reflections with $I_o > 2\sigma(I_o)$ and GOOF = 1.050. Non-hydrogen atoms were anisotropically refined and the hydrogen atoms were placed on calculated positions with temperature factors fixed at 1.2 times U_{eq} of the parent atoms and 1.5 times U_{eq} for methyl groups. The fundamental crystal data and experimental parameters for the structure determination are summarized below.

formula	$C_{24}H_{20}N_4S_6$, C_5H_{12}
M (gmol^{-1})	600.89
crystal dimensions (mm^3)	0.5x0.3x0.15
crystal system	monoclinic
space group	*C*2/c
a (Å)	14.5105(5)
b (Å)	13.5453(6)
c (Å)	15.6906(5)
β (deg)	104.689(7)
V (Å^3)	2864.96(18)
Z	4
ρ_{calc} (gcm^{-3})	1.393
$2\theta_{max}$ (deg)	70.45
radiation	CuKα
λ (Å)	1.54178
F(000)	1256
T (K)	100(2)
measured reflections	13282
unique reflections	2692
observed reflections ($I_o > 2\sigma(I_o)$)	2283
parameters refined	375
R_1	0.0480
ωR_2[a]	0.0999
R_1 (all data)	0.0480
ωR_2 (all data)	0.1067
GOOF	1.050
μ (mm^{-1})	4.601

[a] Weighting scheme as defined for this component: $\omega = 1 / [\sigma^2(F_o^2) + (0.0000\ P)^2 + 0.3014\ P]$, $P = (F_o^2 + 2F_c^2) / 3$

The electrophilic character of the pyrimidine rings (mainly conjugation to the neighboring pyrimidine components) is less pronounced, as the difference between the C-S bonds is only 0.013 Å shorter on the pyrimidine (<1,764 Å> (range 1.763(3)–1.765(3) Å) vs. <1.777 Å> (range 1.776(2)–1.778(2) Å)) side of the bridging sulfur atoms. The calixarene is situated on a 2-fold rotational axis, with the opposite phenyl rings at an angle of 30.9° and the SMe groups on the pyrimidine rings pointing away from the calixarene centre (Figure S2). Short contacts (3.599(1) Å) between a bridging S atom and a neighboring S from a SMe group are observed. For the same bridging S atom, a weak hydrogen contact is observed

with a methyl hydrogen atom of another neighboring SMe group. A pentane molecule is trapped in the crystal structure and is also positioned onto a 2-fold axis.

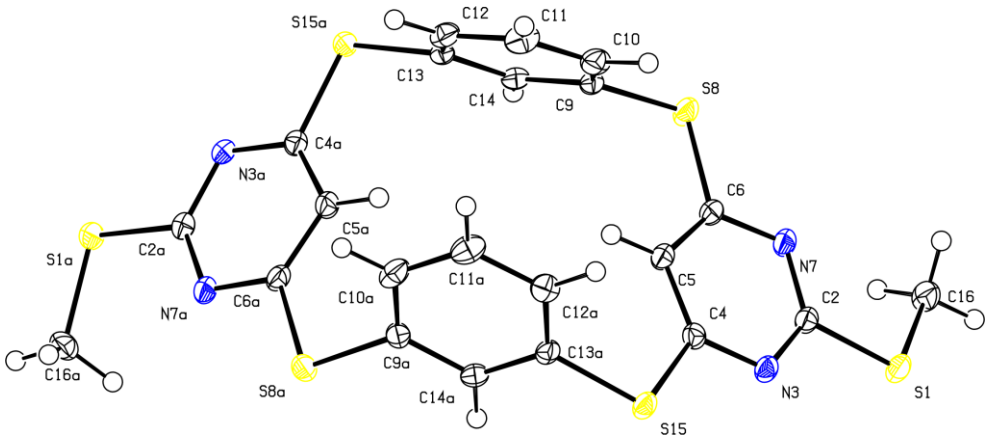

Figure S2. Single-crystal structure for thiacalix[4]arene **6**, showing displacement ellipsoids drawn at the 50% probability level (pentane not shown).

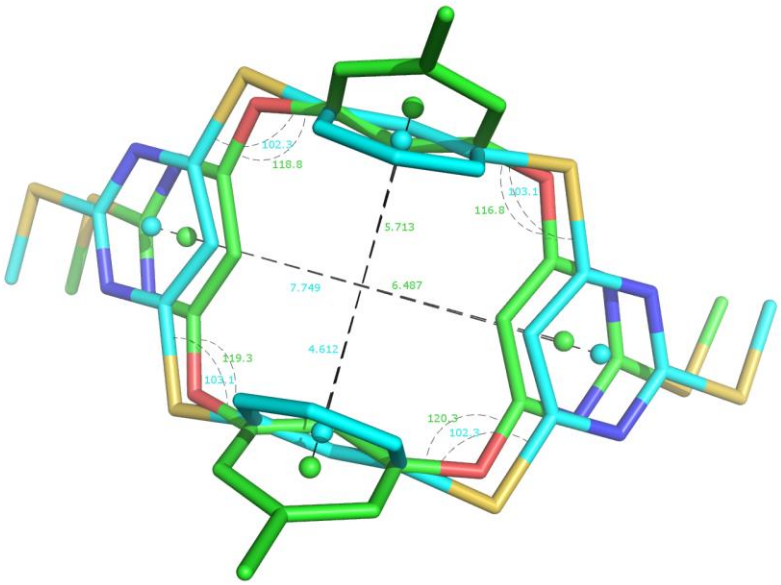

Figure S3. Overlay of the single-crystal structures for oxacalix[4]arene **3** (green backbone) and thiacalix[4]arene **6** (blue backbone), with an indication of centroid-centroid distances and C-X-C bond angles.

Crystallographic data (excluding structure factors) for the structures reported in this paper have been deposited with the Cambridge Crystallographic Data Centre as supplementary publication no. **CCDC-843478** and **843479**. Copies of the data can be obtained free of charge on application to CCDC, 12 Union Road, Cambridge CB2 1EZ, UK (fax: +44(0)-1223-336033 or e-mail: deposit@ccdc.cam.ac.uk).

3. Variable temperature NMR data

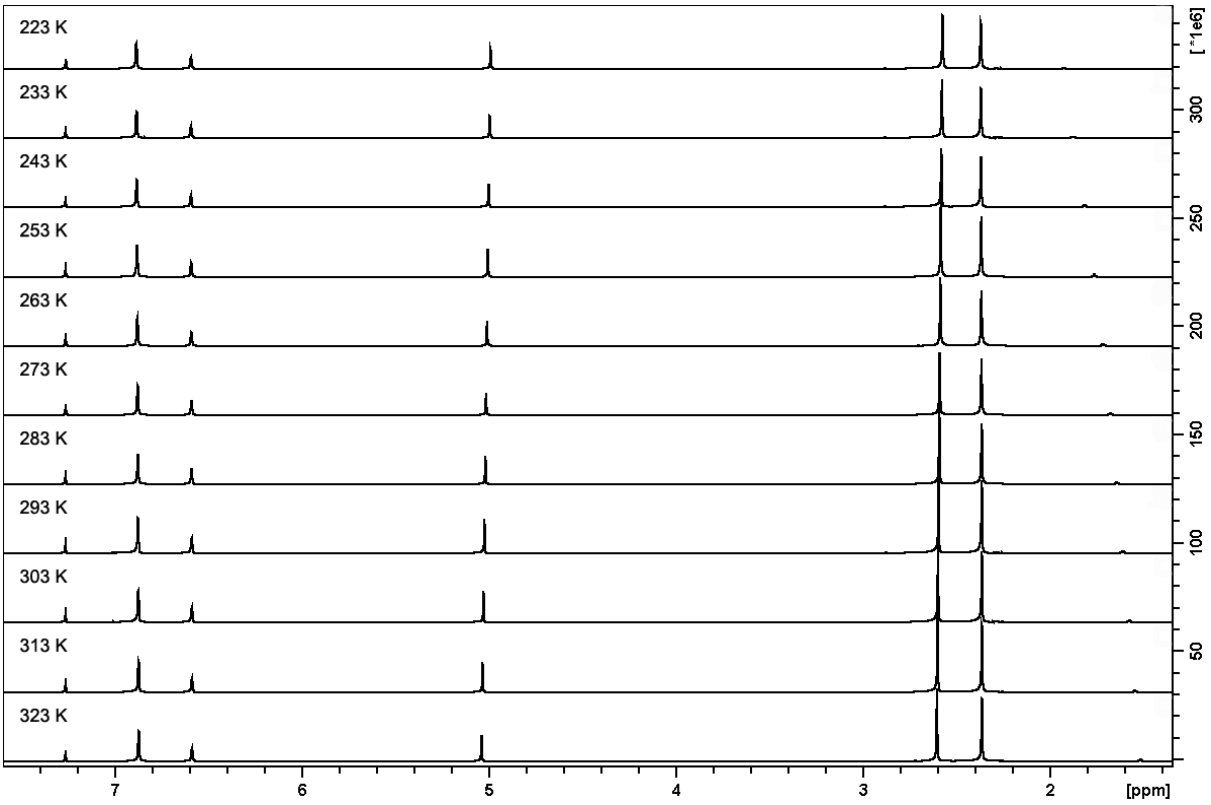

Figure S4. VT-NMR analysis of bis(methylsulfanyl)oxacalix[2]arene[2]pyrimidine **3** in $CDCl_3$.

4. Additional data on the ^{1}H NMR titrations

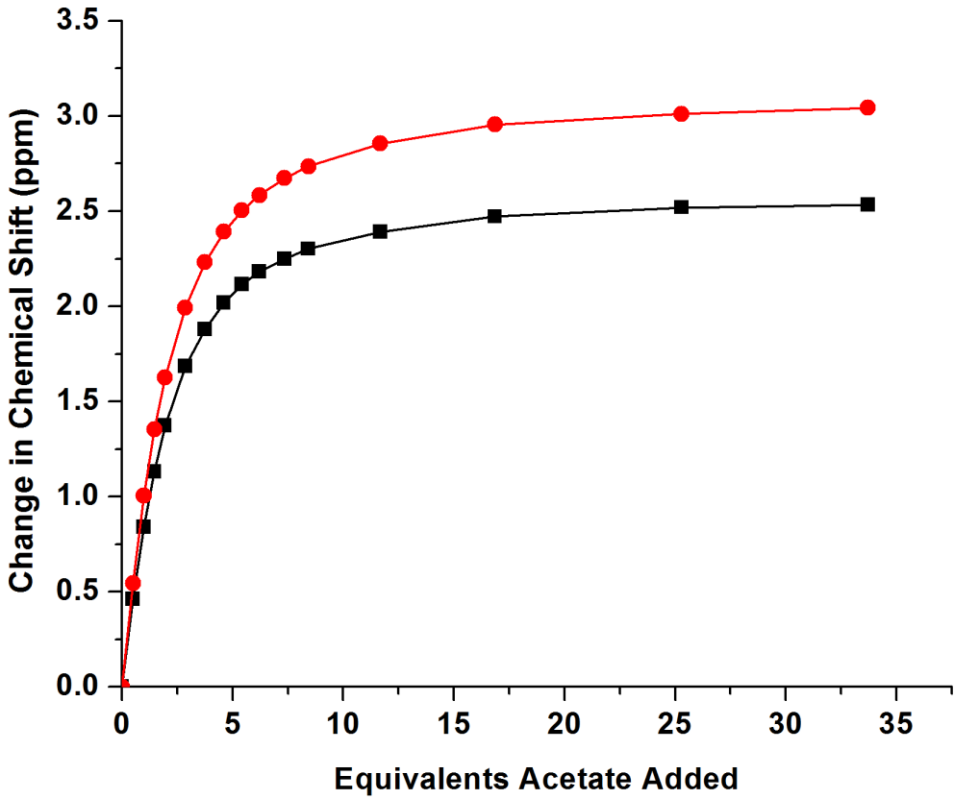

Figure S5. ^{1}H NMR titration curve of host **10a** (0.5 mL, 5×10^{-3} M in DMSO-d_6/0.5% H_2O): variation of chemical shift of NH_a (black) and NH_b (red) vs. equiv tetra-*n*-butylammonium acetate added.

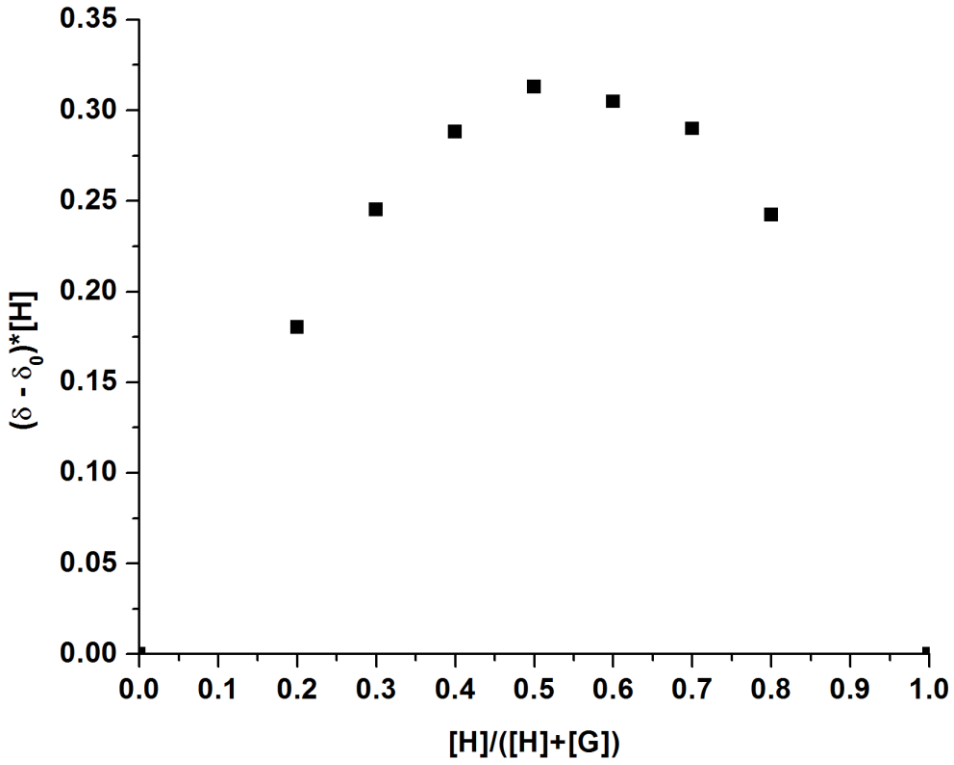

Figure S6. Job plot for the complexation of host **10a** (5×10^{-3} M) with tetra-*n*-butylammonium acetate in DMSO-d_6/0.5% H_2O.

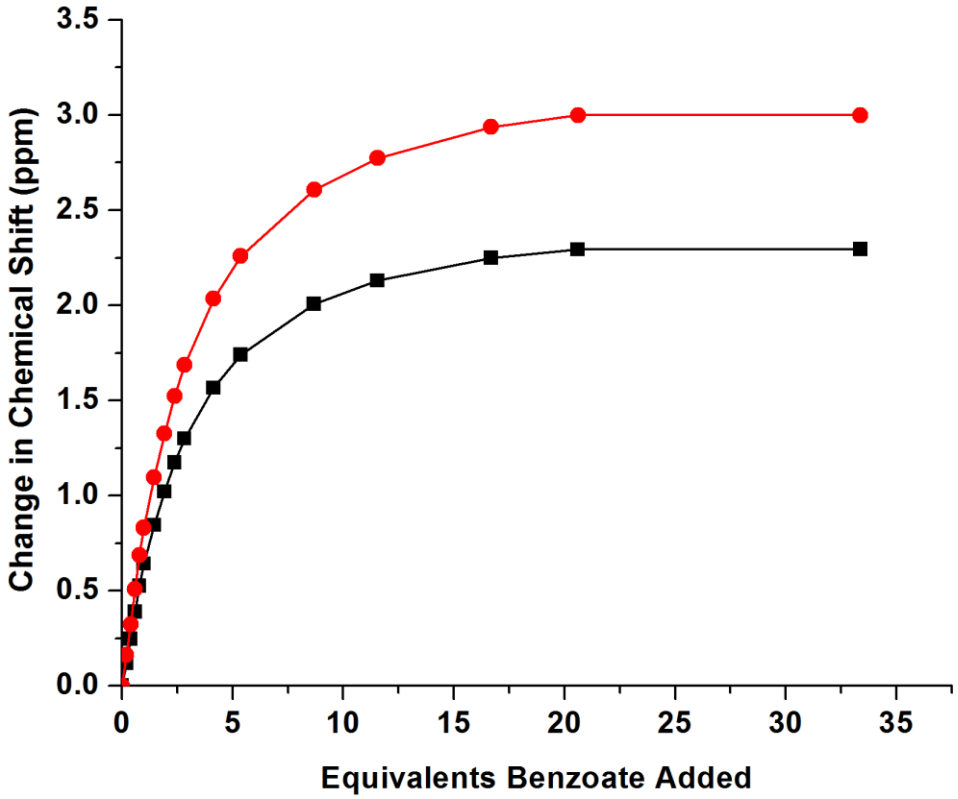

Figure S7. ^{1}H NMR titration curve of host **10a** (0.5 mL, 5×10^{-3} M in DMSO-d_6/0.5% H_2O): variation of chemical shift of NH_a (black) and NH_b (red) vs. equiv tetra-*n*-butylammonium benzoate added.

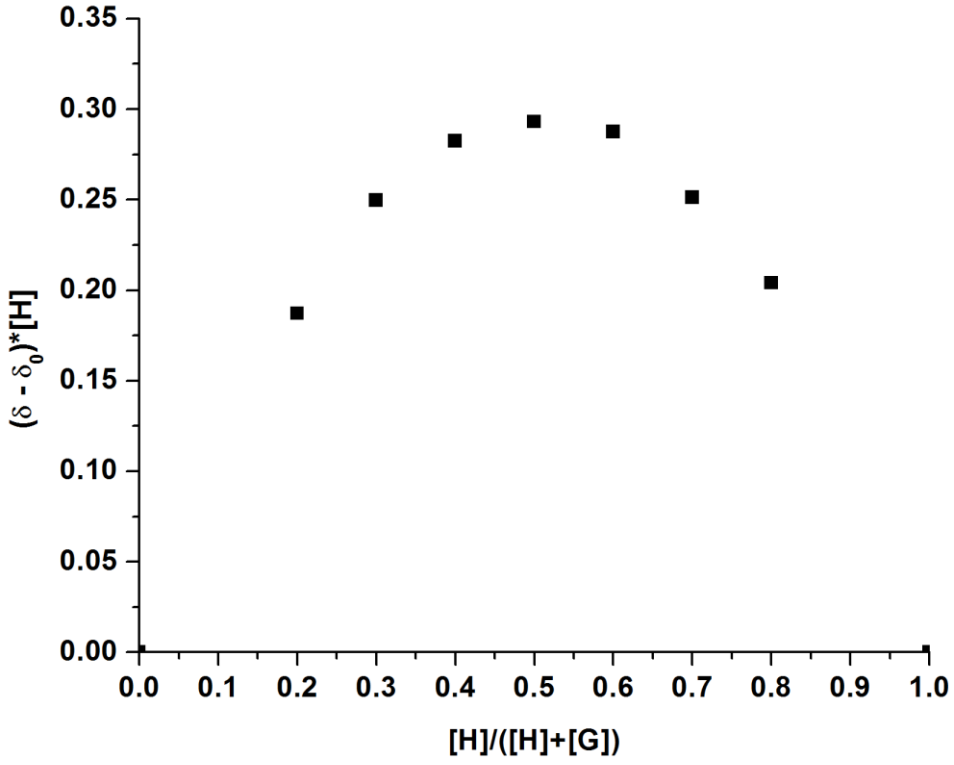

Figure S8. Job plot for the complexation of host **10a** (5×10^{-3} M) with tetra-*n*-butylammonium benzoate in DMSO-d_6/0.5% H_2O.

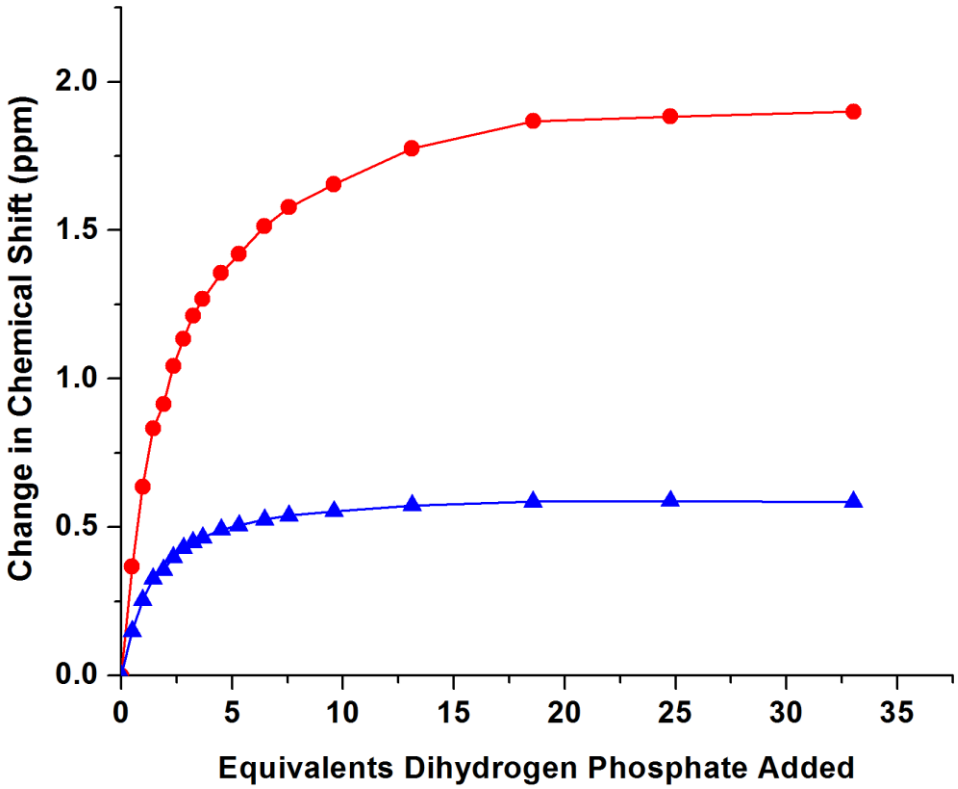

Figure S9. ^{1}H NMR titration curve of host **10a** (0.5 mL, 5×10^{-3} M in DMSO-d_6/0.5% H_2O): variation of chemical shift of NH_b (red) and NH_c (blue) vs. equiv tetra-*n*-butylammonium dihydrogen phosphate added.

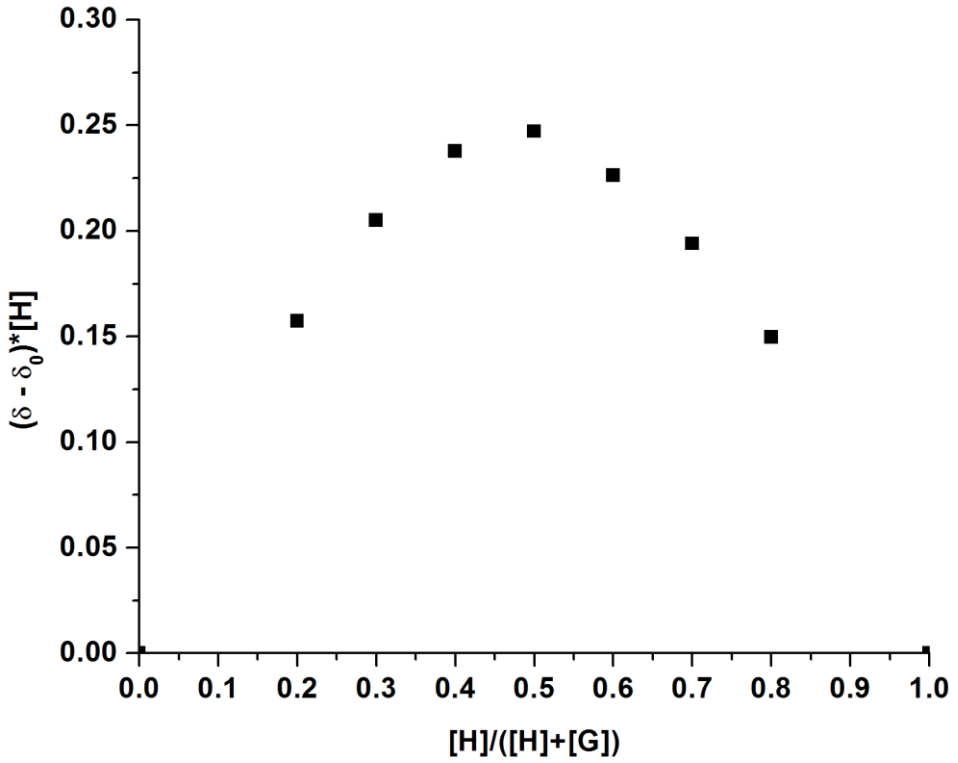

Figure S10. Job plot for the complexation of host **10a** (5×10^{-3} M) with tetra-*n*-butylammonium dihydrogen phosphate in DMSO-d_6/0.5% H_2O.

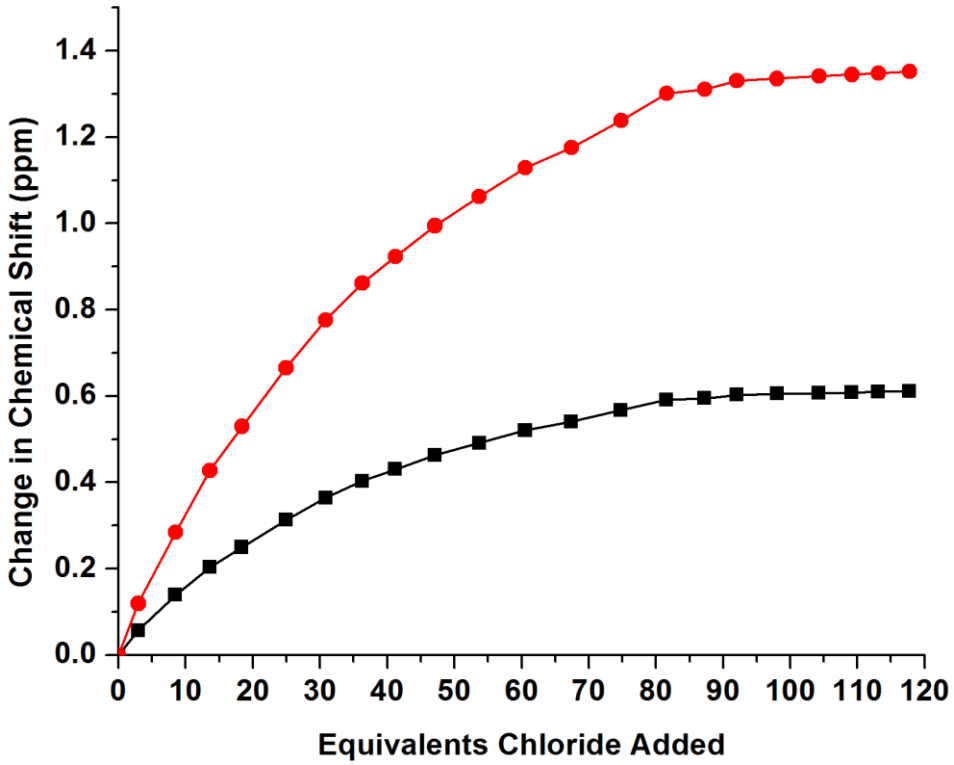

Figure S11. ^{1}H NMR titration curve of host **10a** (0.5 mL, 5×10^{-3} M in DMSO-d_6/0.5% H_2O): variation of chemical shift of NH_a (black) and NH_b (red) vs. equiv tetra-*n*-butylammonium chloride added.

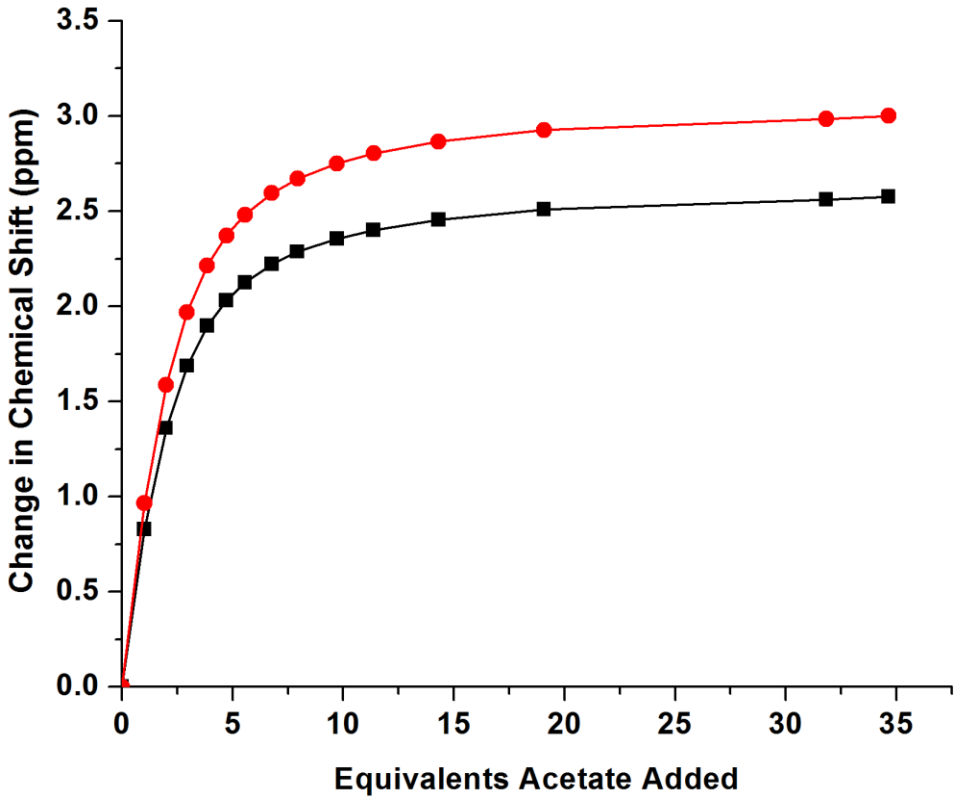

Figure S12. ^{1}H NMR titration curve of host **10b** (0.5 mL, 5×10^{-3} M in DMSO-d_6/0.5% H_2O): variation of chemical shift of NH_a (black) and NH_b (red) vs. equiv tetra-*n*-butylammonium acetate added.

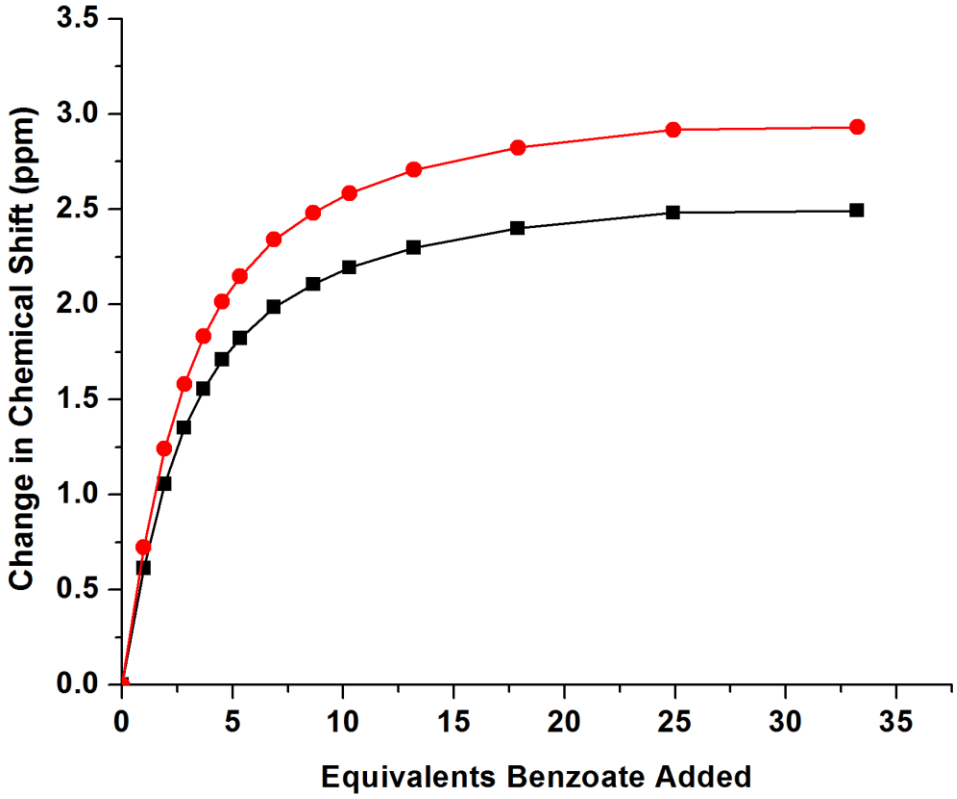

Figure S13. ^{1}H NMR titration curve of host **10b** (0.5 mL, 5×10^{-3} M in DMSO-d_6/0.5% H_2O): variation of chemical shift of NH_a (black) and NH_b (red) vs. equiv tetra-*n*-butylammonium benzoate added.

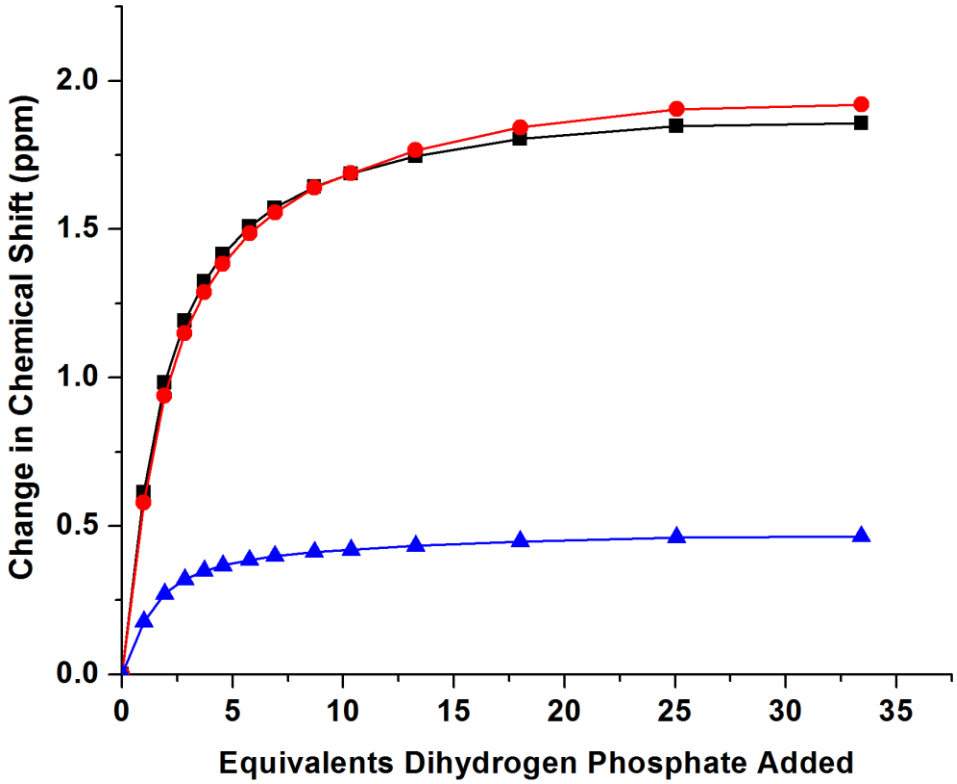

Figure S14. ^{1}H NMR titration curve of host **10b** (0.5 mL, 5×10^{-3} M in DMSO-d_6/0.5% H_2O): variation of chemical shift of NH_a (black), NH_b (red) and NH_c (blue) vs. equiv tetra-*n*-butylammonium dihydrogen phosphate added.

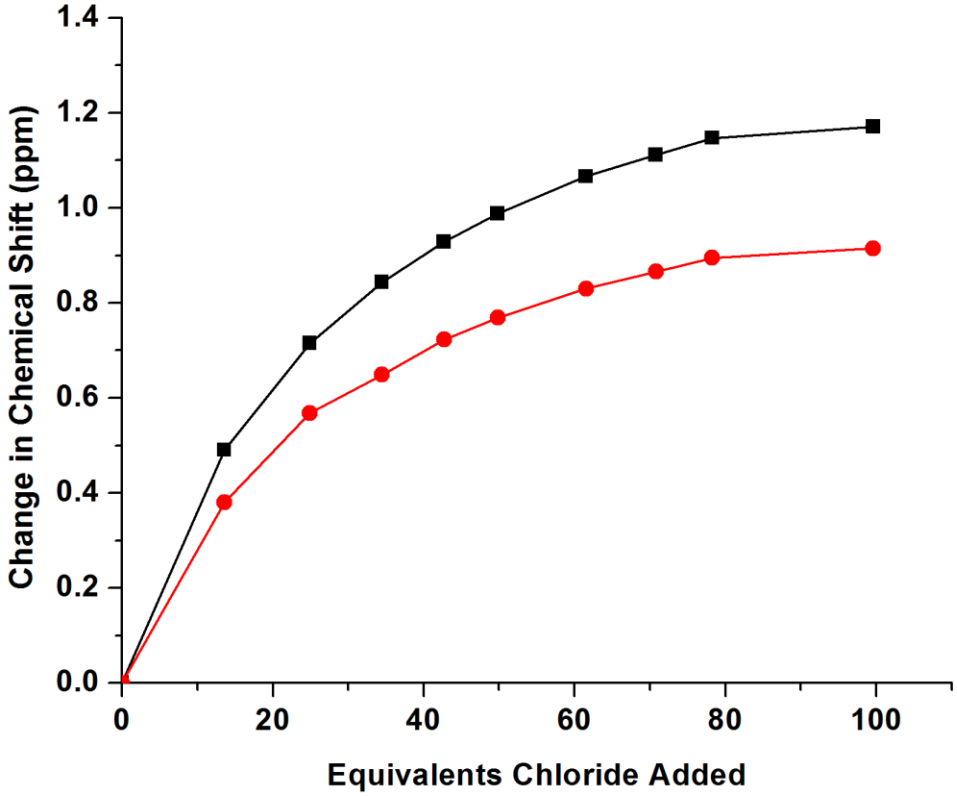

Figure S15. ^{1}H NMR titration curve of host **10b** (0.5 mL, 5×10^{-3} M in DMSO-d_6/0.5% H_2O): variation of chemical shift of NH_a (black) and NH_b (red) vs. equiv tetra-*n*-butylammonium chloride added.

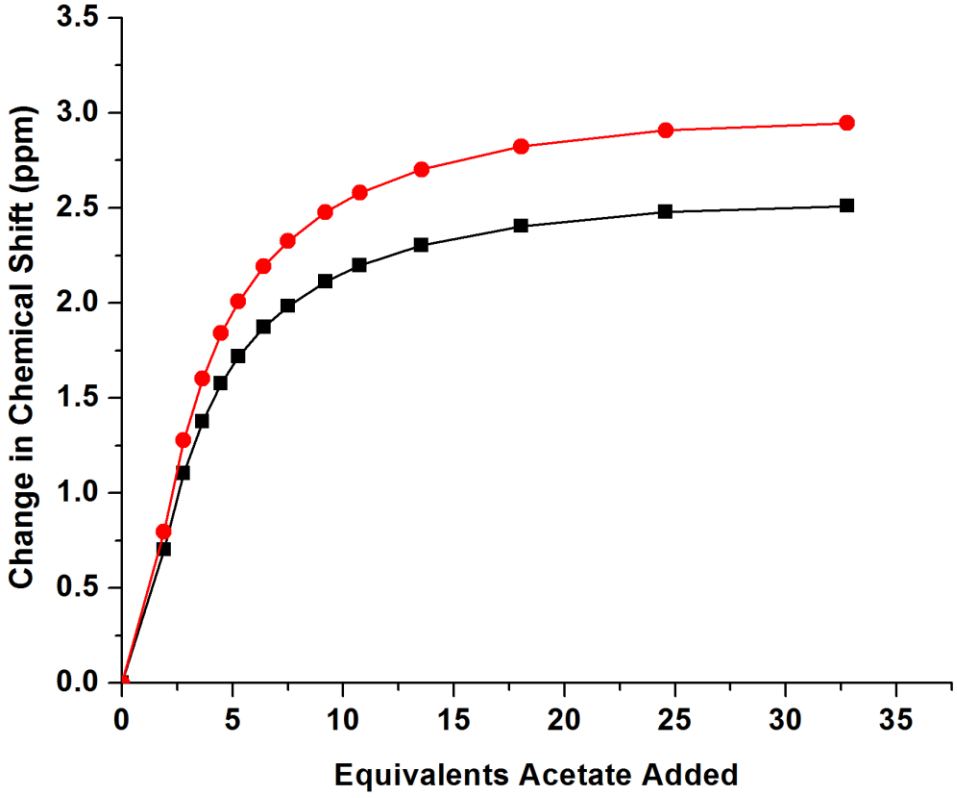

Figure S16. ^{1}H NMR titration curve of host **10c** (0.5 mL, 5×10^{-3} M in DMSO-d_6/0.5% H_2O): variation of chemical shift of NH_a (black) and NH_b (red) vs. equiv tetra-*n*-butylammonium acetate added.

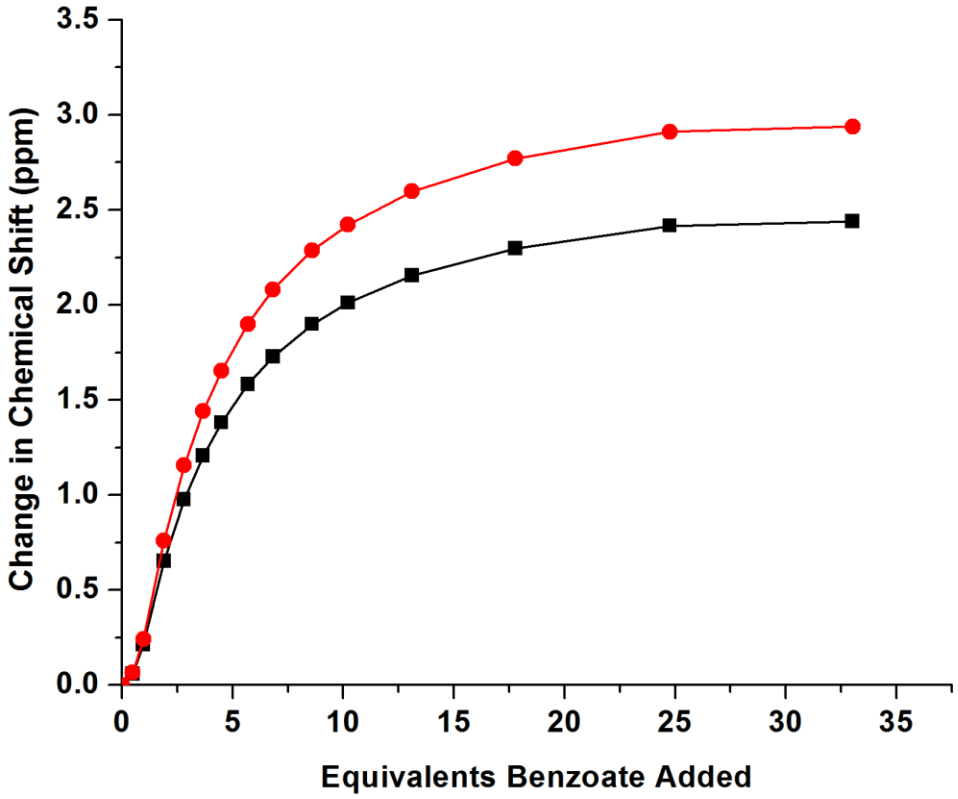

Figure S17. ^{1}H NMR titration curve of host **10c** (0.5 mL, 5×10^{-3} M in DMSO-d_6/0.5% H_2O): variation of chemical shift of NH_a (black) and NH_b (red) vs. equiv tetra-*n*-butylammonium benzoate added.

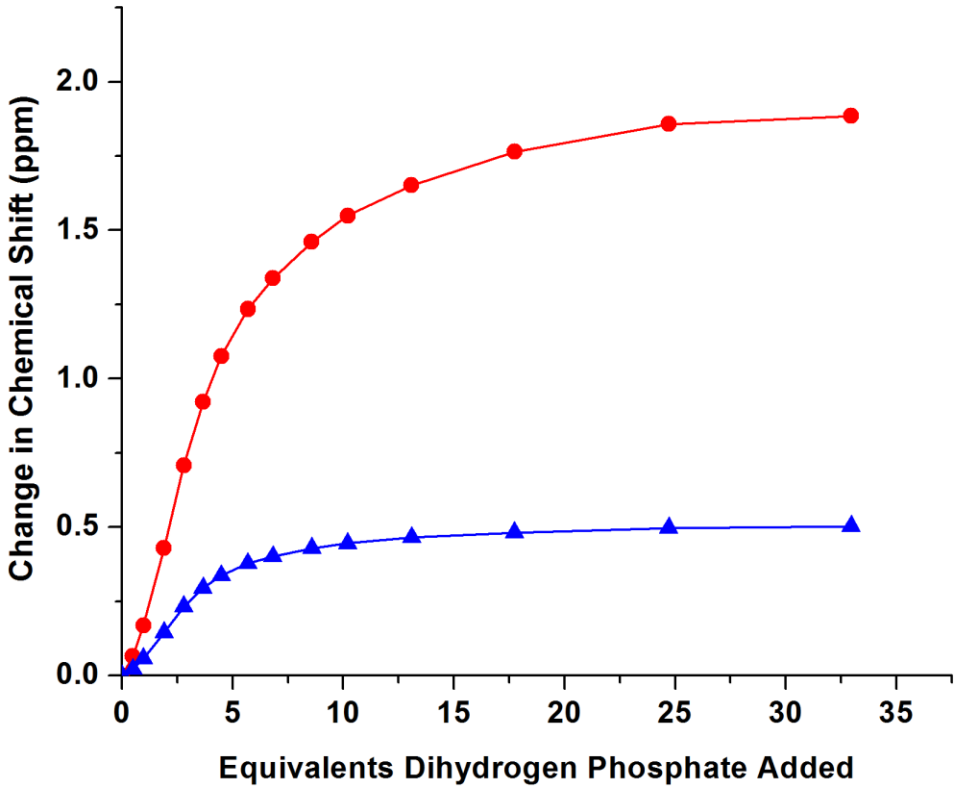

Figure S18. ^{1}H NMR titration curve of host **10c** (0.5 mL, 5×10^{-3} M in DMSO-d_6/0.5% H_2O): variation of chemical shift of NH_b (red) and NH_c (blue) vs. equiv tetra-*n*-butylammonium dihydrogen phosphate added.

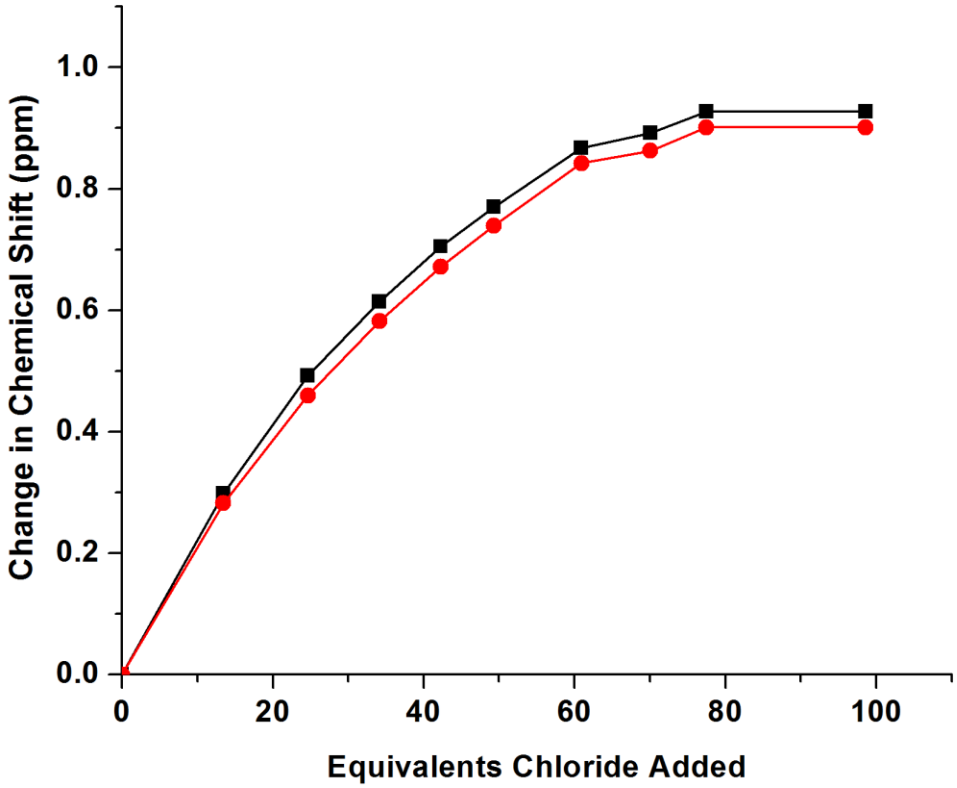

Figure S19. ^{1}H NMR titration curve of host **10c** (0.5 mL, 5×10^{-3} M in DMSO-d_6/0.5% H_2O): variation of chemical shift of NH_a (black) and NH_b (red) vs. equiv tetra-*n*-butylammonium chloride added.

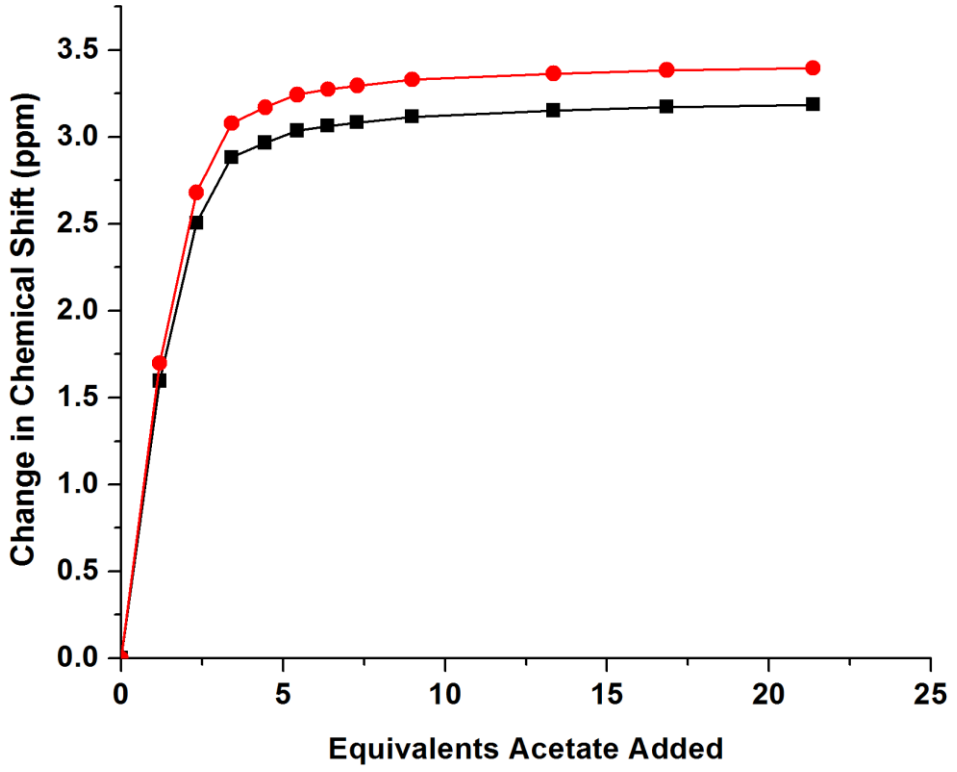

Figure S20. ^{1}H NMR titration curve of host **10d** (0.5 mL, 5×10^{-3} M in DMSO-d_6/0.5% H_2O): variation of chemical shift of NH_a (black) and NH_b (red) vs. equiv tetra-*n*-butylammonium acetate added.

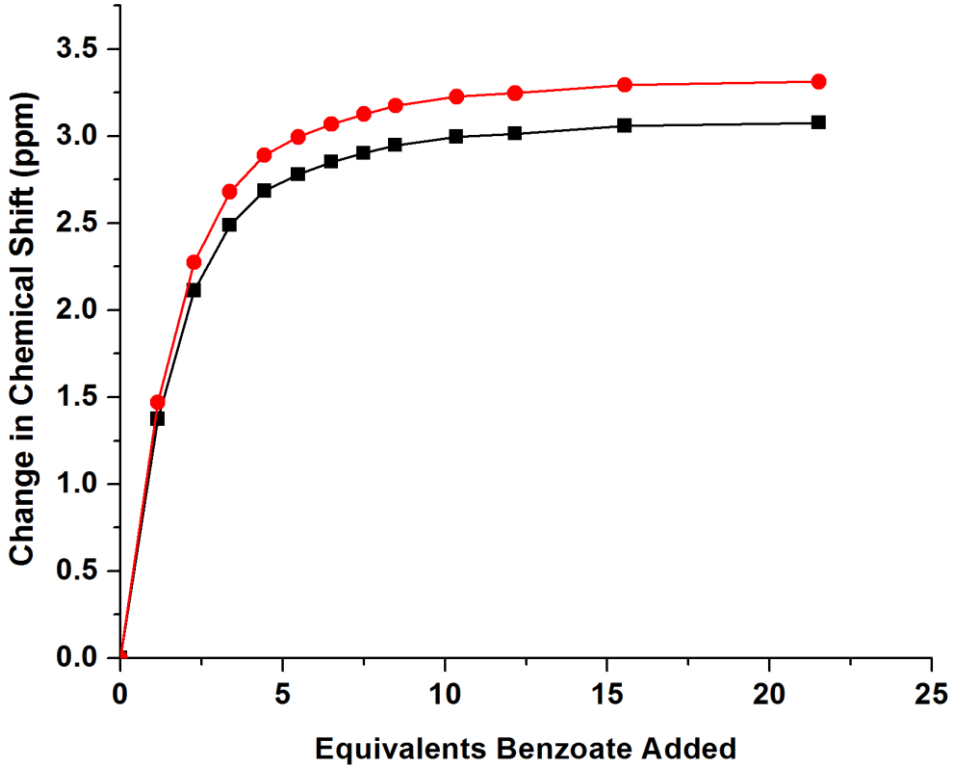

Figure S21. ^{1}H NMR titration curve of host **10d** (0.5 mL, 5×10^{-3} M in DMSO-d_6/0.5% H_2O): variation of chemical shift of NH_a (black) and NH_b (red) vs. equiv tetra-*n*-butylammonium benzoate added.

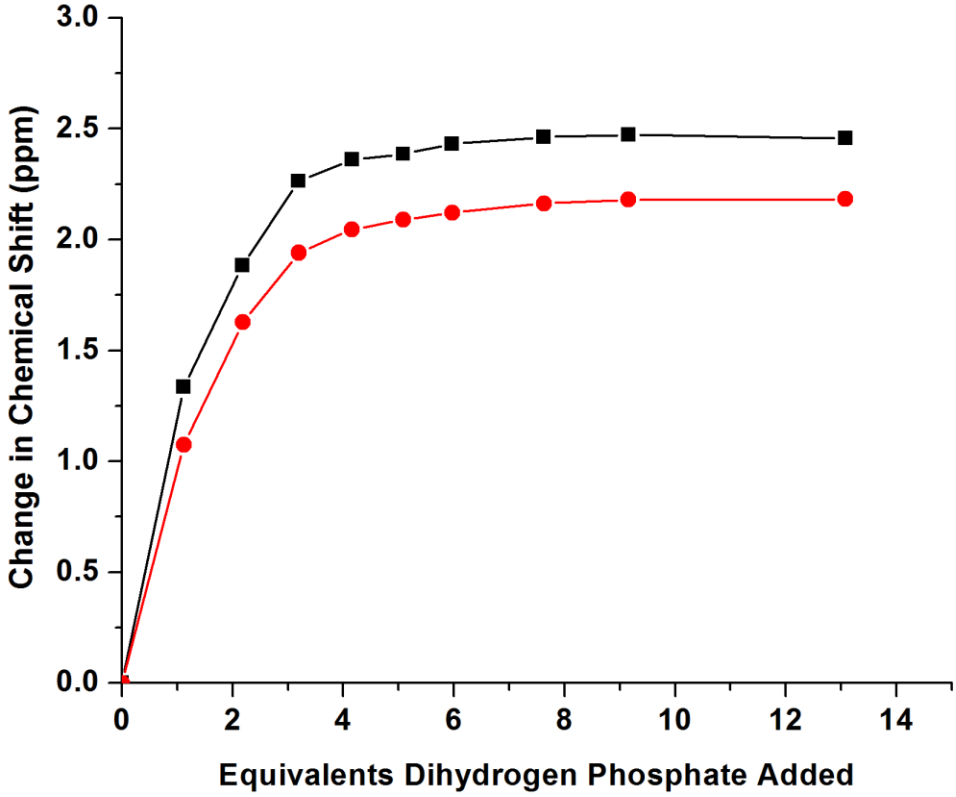

Figure S22. ^{1}H NMR titration curve of host **10d** (0.5 mL, 5×10^{-3} M in DMSO-d_6/0.5% H_2O): variation of chemical shift of NH_a (black) and NH_b (red) vs. equiv tetra-*n*-butylammonium dihydrogen phosphate added.

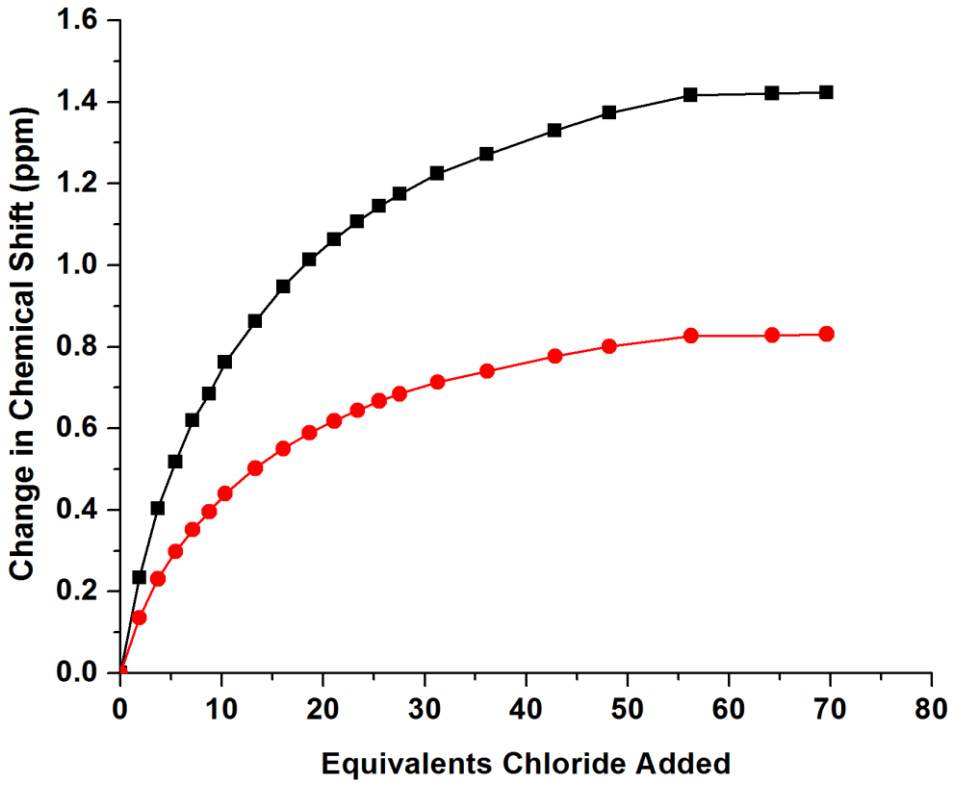

Figure S23. ^{1}H NMR titration curve of host **10d** (0.5 mL, 5×10^{-3} M in DMSO-d_6/0.5% H_2O): variation of chemical shift of NH_a (black) and NH_b (red) vs. equiv tetra-*n*-butylammonium chloride added.

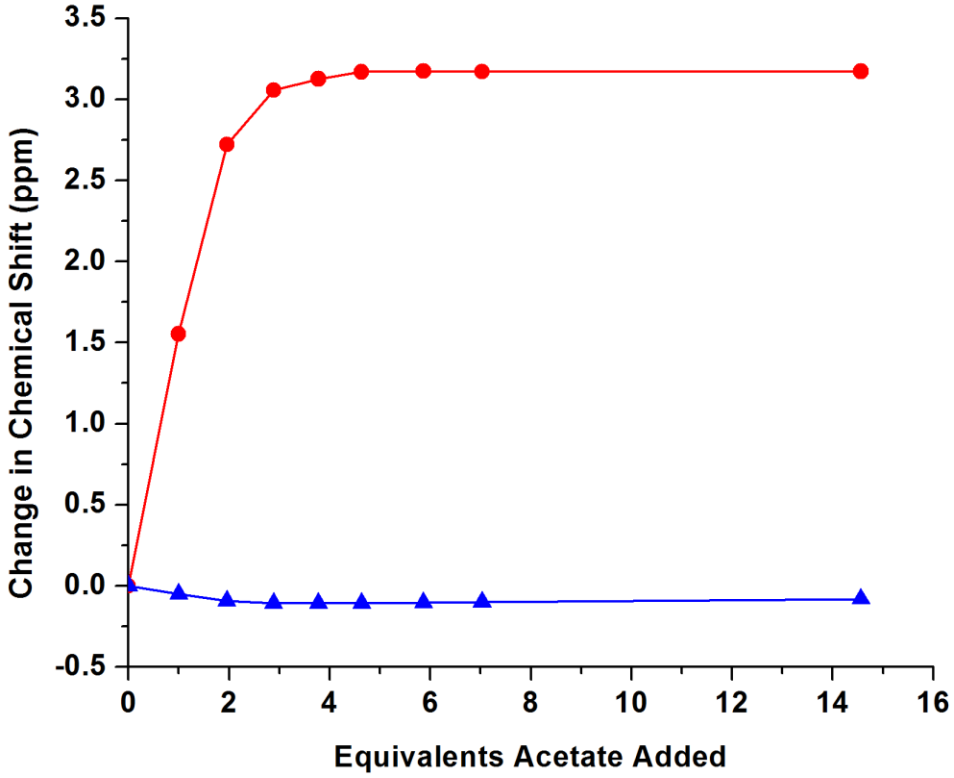

Figure S24. ^{1}H NMR titration curve of host **10e** (0.5 mL, 5×10^{-3} M in DMSO-d_6/0.5% H_2O): variation of chemical shift of NH_b (red) and NH_c (blue) vs. equiv tetra-*n*-butylammonium acetate added.

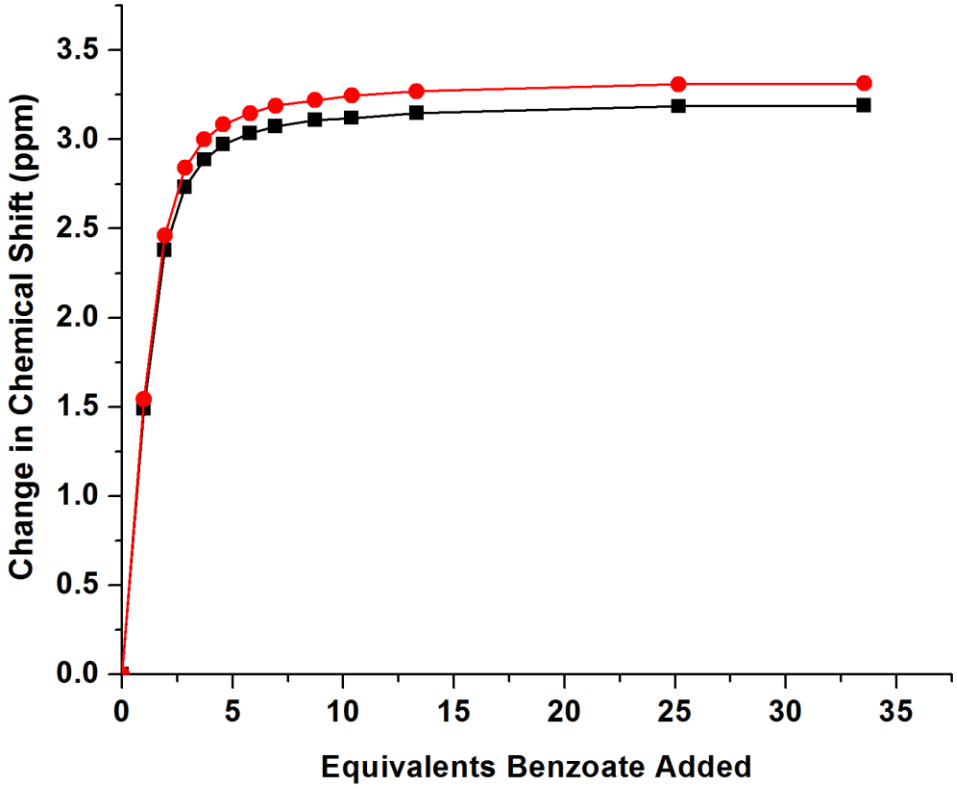

Figure S25. ^{1}H NMR titration curve of host **10e** (0.5 mL, 5×10^{-3} M in DMSO-d_6/0.5% H_2O): variation of chemical shift of NH_a (black) and NH_b (red) vs. equiv tetra-*n*-butylammonium benzoate added.

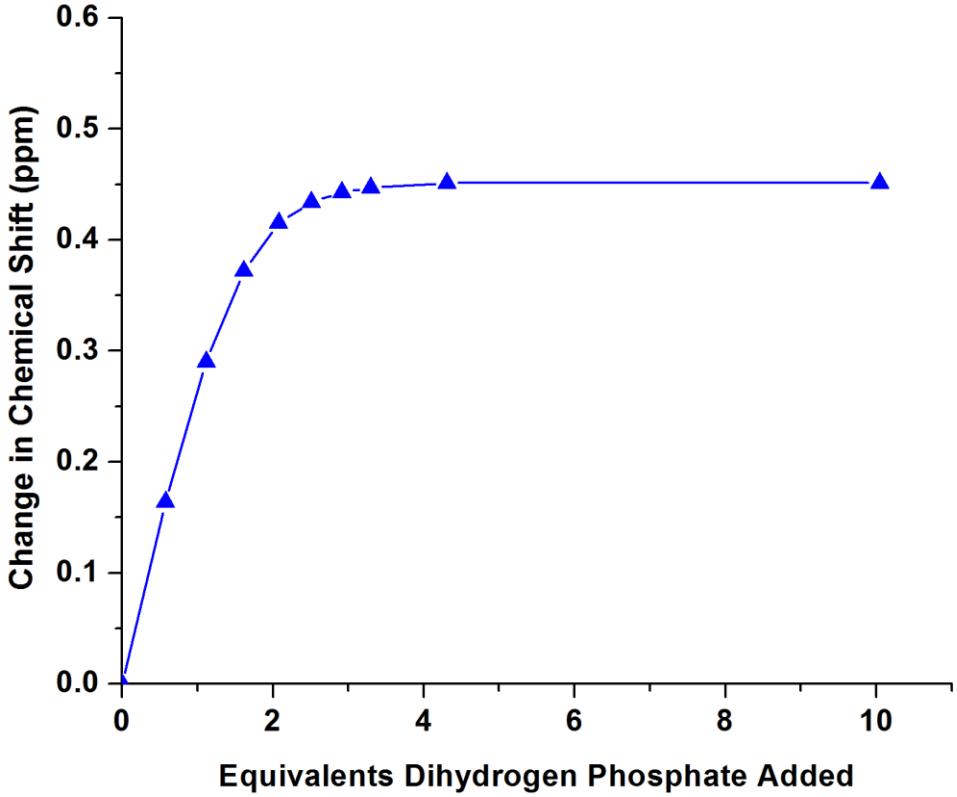

Figure S26. ^{1}H NMR titration curve of host **10e** (0.5 mL, 5×10^{-3} M in DMSO-d_6/0.5% H_2O): variation of chemical shift of NH_c (blue) vs. equiv tetra-*n*-butylammonium dihydrogen phosphate added.

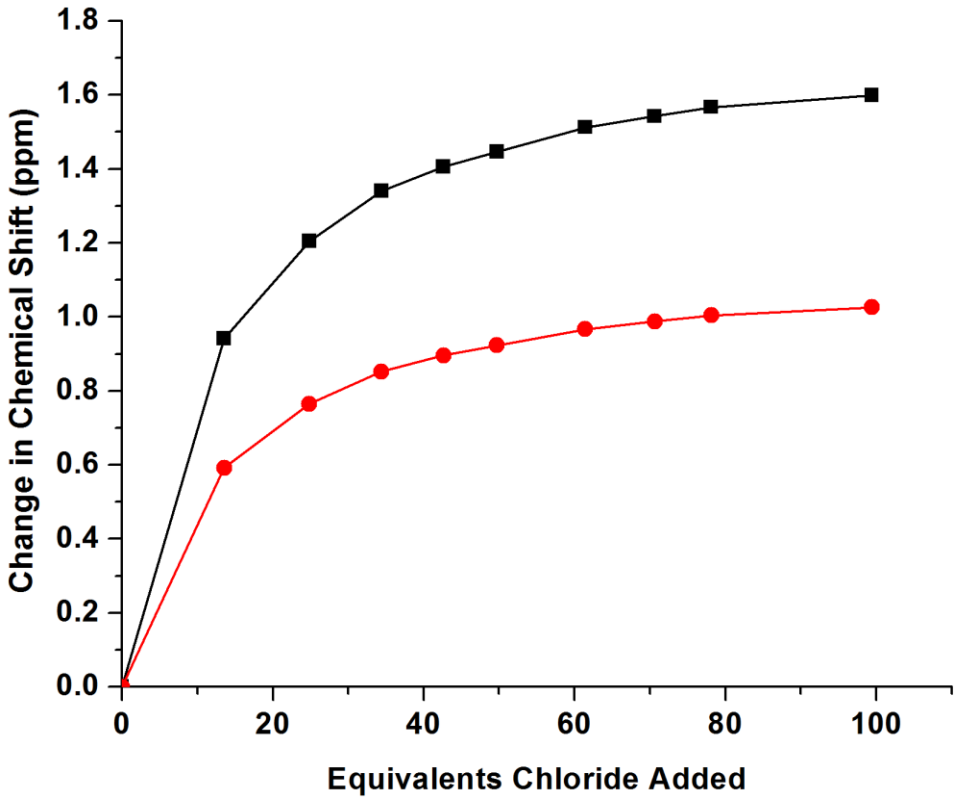

Figure S27. ^{1}H NMR titration curve of host **10e** (0.5 mL, 5×10^{-3} M in DMSO-d_6/0.5% H_2O): variation of chemical shift of NH_a (black) and NH_b (red) vs. equiv tetra-*n*-butylammonium chloride added.

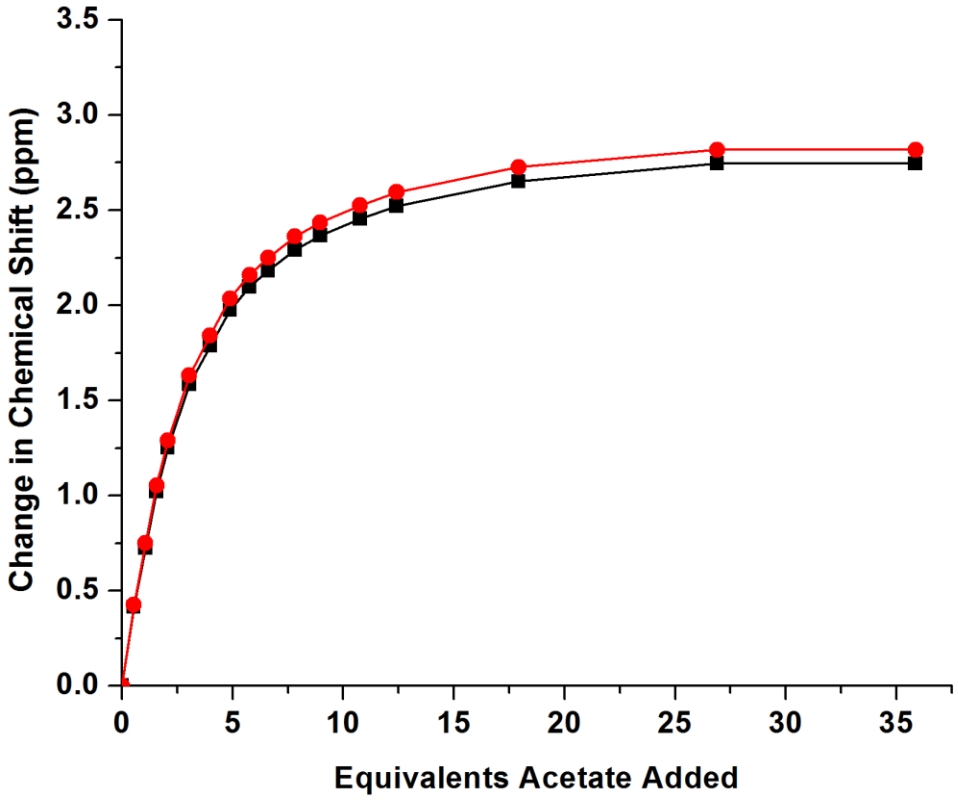

Figure S28. ^{1}H NMR titration curve of host **10f** (0.5 mL, 5×10^{-3} M in DMSO-d_6/0.5% H_2O): variation of chemical shift of NH_a (black) and NH_b (red) vs. equiv tetra-*n*-butylammonium acetate added.

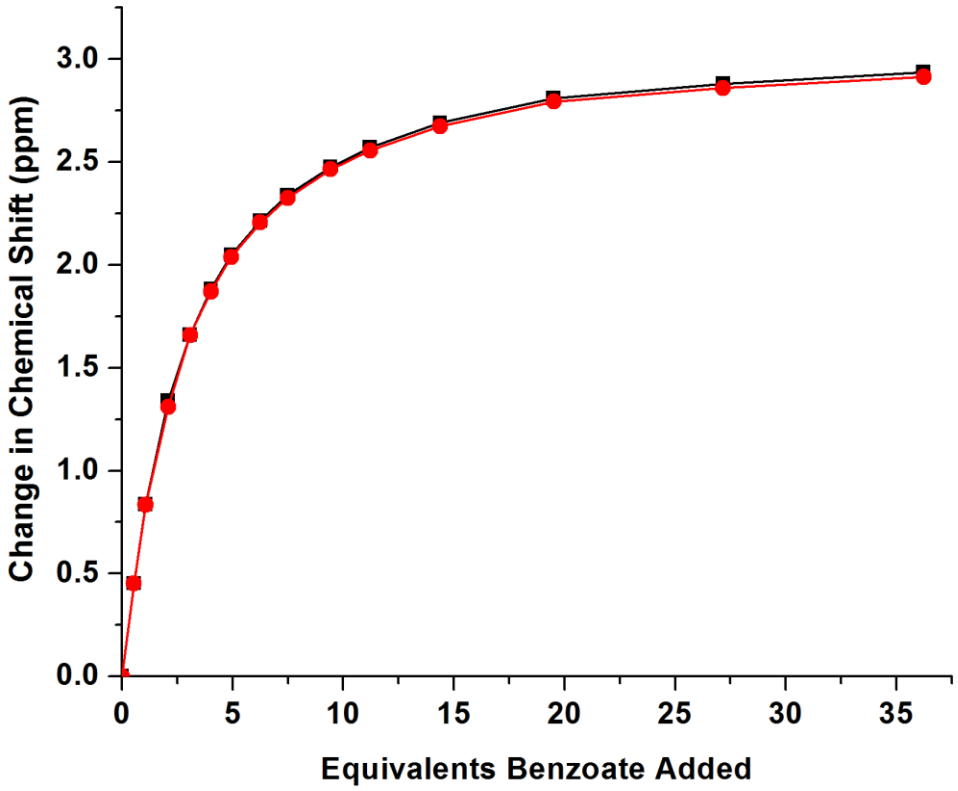

Figure S29. ^{1}H NMR titration curve of host **10f** (0.5 mL, 5×10^{-3} M in DMSO-d_6/0.5% H_2O): variation of chemical shift of NH_a (black) and NH_b (red) vs. equiv tetra-*n*-butylammonium benzoate added.

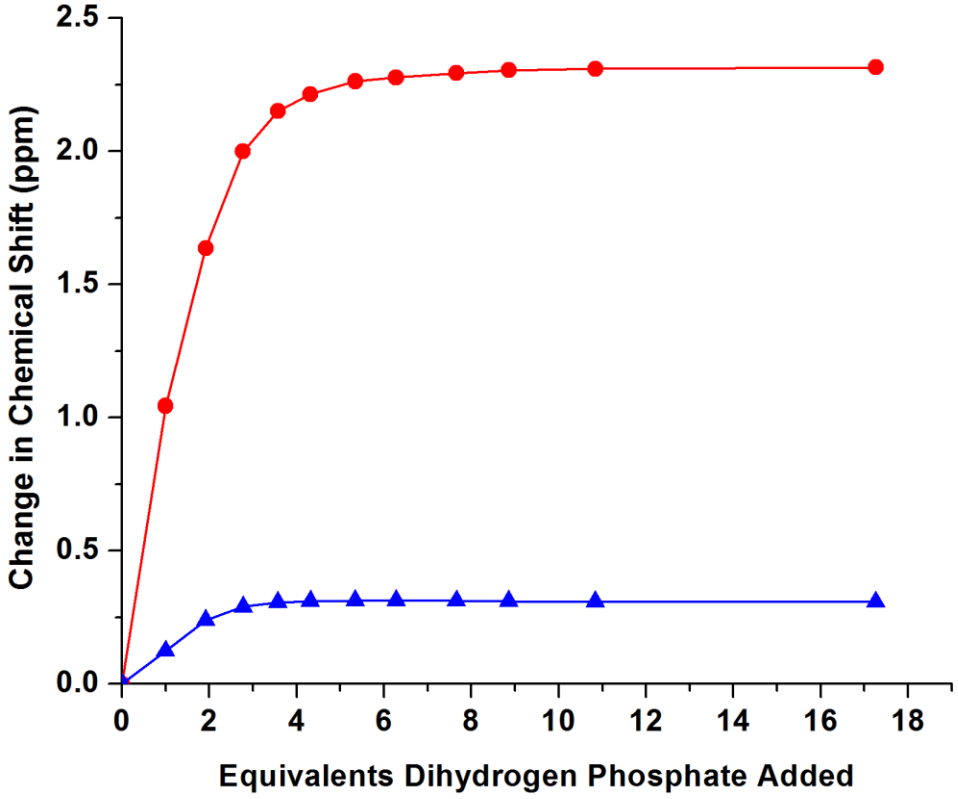

Figure S30. ^{1}H NMR titration curve of host **10f** (0.5 mL, 5×10^{-3} M in DMSO-d_6/0.5% H_2O): variation of chemical shift of NH_b (red) and NH_c (blue) vs. equiv tetra-*n*-butylammonium dihydrogen phosphate added.

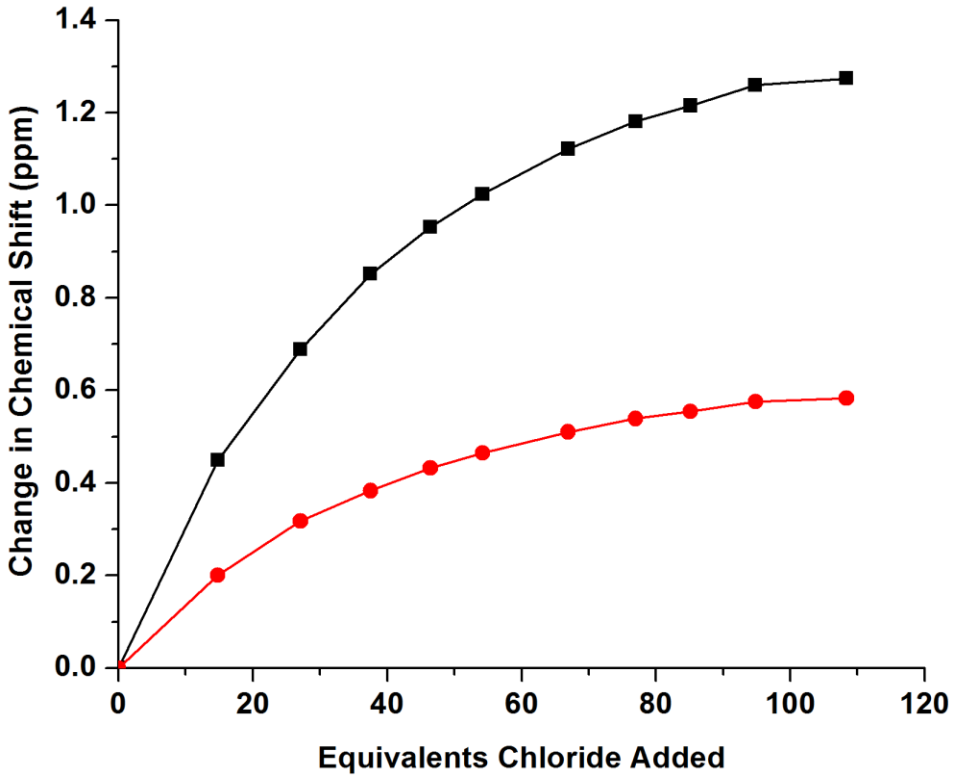

Figure S31. ^{1}H NMR titration curve of host **10f** (0.5 mL, 5×10^{-3} M in DMSO-d_6/0.5% H_2O): variation of chemical shift of NH_a (black) and NH_b (red) vs. equiv tetra-*n*-butylammonium chloride added.

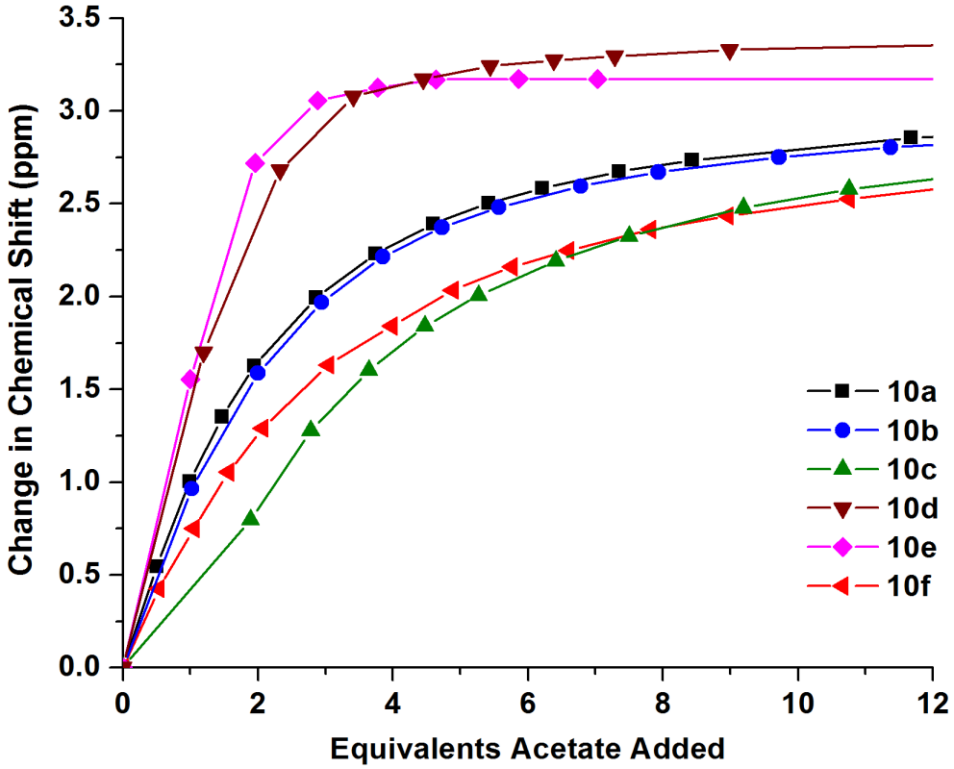

Figure S32. ^{1}H NMR titration curve of hosts **10a–f** (0.5 mL, 5×10^{-3} M in DMSO-d_6/0.5% H_2O): overview of the variation of the chemical shift of NH_b vs. equiv tetra-*n*-butylammonium acetate added.

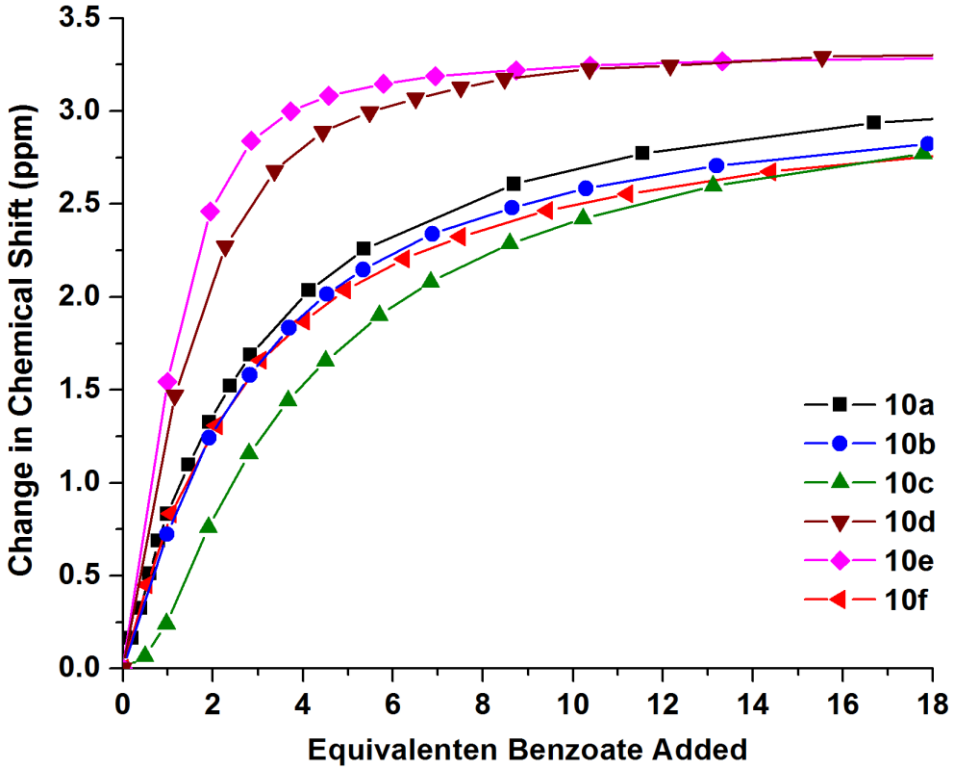

Figure S33. ^{1}H NMR titration curve of hosts **10a–f** (0.5 mL, 5×10^{-3} M in DMSO-d_6/0.5% H_2O): overview of the variation of the chemical shift of NH_b vs. equiv tetra-*n*-butylammonium benzoate added.

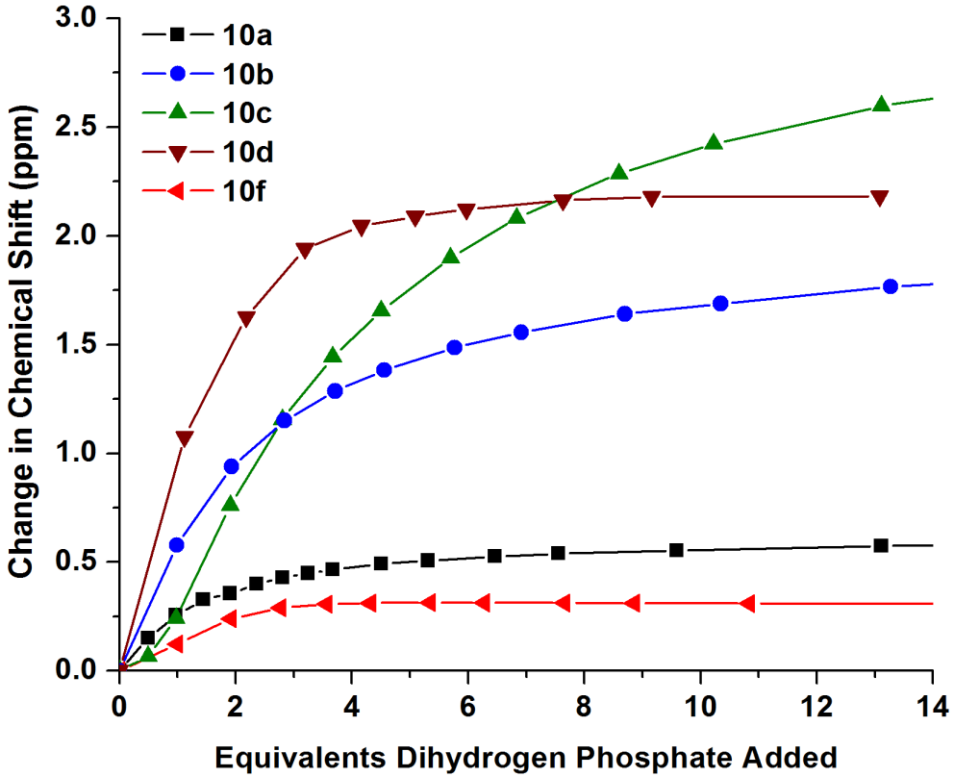

Figure S34. ^{1}H NMR titration curve of hosts **10a–f** (0.5 mL, 5×10^{-3} M in DMSO-d_6/0.5% H_2O): overview of the variation of the chemical shift of NH_b vs. equiv tetra-*n*-butylammonium dihydrogen phosphate added.

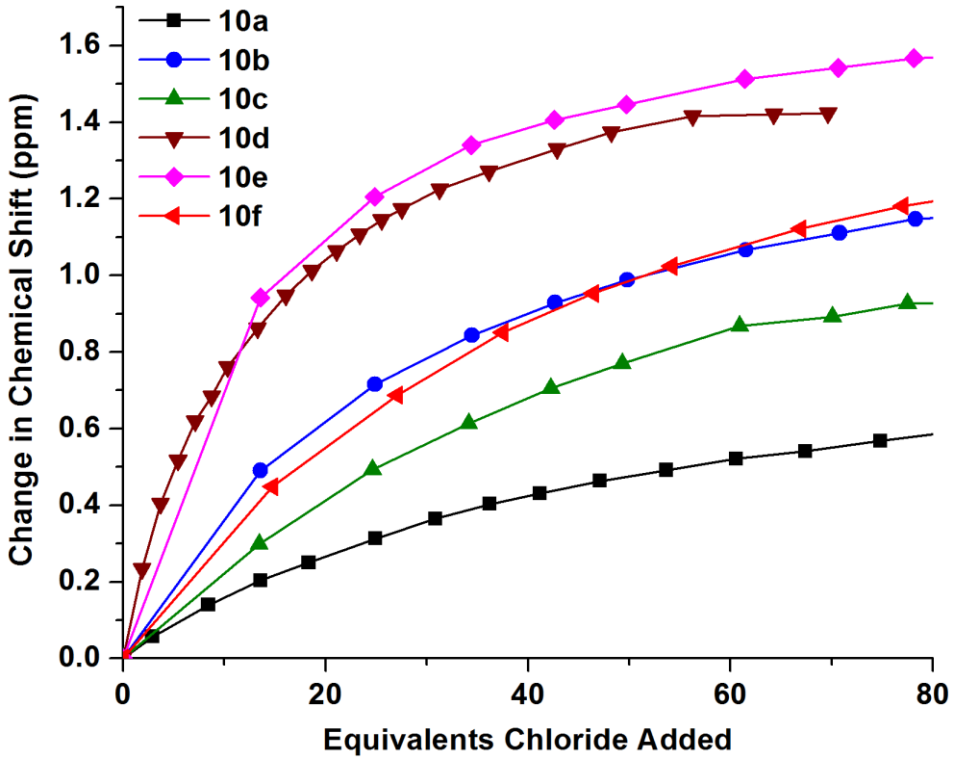

Figure S35. ^{1}H NMR titration curve of hosts **10a–f** (0.5 mL, 5×10^{-3} M in DMSO-d_6/0.5% H_2O): overview of the variation of the chemical shift of NH_b vs. equiv tetra-*n*-butylammonium chloride added.